PEOPLE'S DEMOCRATIC REPUBLIC OF ALGERIA

MINISTRY OF HIGHER EDUCATION AND SCIENTIFIC RESEARCH

YAHIA FARES UNIVERSITY OF MEDEA

Faculty of **T**echnology

Department of **E**lectrical **E**ngineering

Master's degree Thesis

Sector : Telecommunications

Specialty : Telecommunications Systems

5G NR Planning: Influence of advanced antenna systems implementation on RF planning predictions

---

Presented by :

KHELIL CHERFI Mohamed

Proposed and directed by :

Dr. GUEDMANI Mohamed

Class of 2022

Acknowledgments

First, I thank Allah for giving me this opportunity to accomplish this work.

I’d like to thank all the people involved, who in a more direct or indirect way, helped me to climb this last step.

الملخص

يهدف الجيل الخامس للاتصالات الى تلبية الاحتياجات المتزايدة و الطلب المتزايد للممستخدمين فيما يتعلق بالسعة و النقل الأني للمعلومات و التي أخذت في التصاعد و الاستمرار مع مرور الوقت بصفة كبيرة جدا. تهدف هاته الأطروحة الى تحليل تأثير الهوائيات المتعددة المداخل و المخارج و تقنية تشكيل الحزم و التي تعد تقنيات واعدة في هذا المجال على الحساب النظري لتنبؤات التغطية التي يستعمل فيها برمجيات خاصة لهذا النوع من الدراسات. تم اجراء هاته الدراسة باستعمال برنامج التخطيط الراديوي اتول من شركة فورسك. تم انجاز دراستين لتقييم تغطية الشبكة, جودتها و سعتها: دراسة مقارنة لأداء الهوائيات النشطة في وضع المستخدم الواحد للشبكة أولا ثم مقارنة الأداء في وضع تعدد المستخدمين للشبكة, أظهرت النتائج و التي استعملت فيها نفس الهوائيات النشطة ذات تقنية تشكيل الحزم العمودية في كافة السيناريوهات المدروسة ردا إيجابيا مقارنة بتقنيات الهوائيات الخاملة المستخدمة من قبل, بينما أثبتت المقارنة بين الهوائيات النشطة في حالة المستخدم الفردي عدم وجود فروقات في التغطية و على العكس من ذلك ففي حالة تعدد المستخدمين و الذي يحاكي الاستخدام الفعلي للشبكة لاحظنا أن استعمال عدد أكبر من مداخل و مخارج الهوائيات ذات الحزم المشكلة أدى الى زيادة في سعة الشبكة و قدرة أكبر على استيعاب المستخدمين لها.

كلمات مفتاحية

هوائيات متعددة المداخل و المخارج, تشكيل الحزم, محاكاة تغطية, سعة

Résumé

La cinquième génération de communications mobiles, la 5G, vise à répondre aux besoins croissants et à la demande accrue des utilisateurs en matière de capacité et de latence, dans une croissance qui a été exponentielle et qui devrait se poursuivre. Cette thèse vise à analyser l'impact des antennes MIMO et de formation de faisceaux dont la technologie est prometteuse pour répondre aux exigences sur les performances du réseau, à travers des prédictions. Cette évaluation a été réalisée à l'aide de l'outil de planification du réseau radio Atoll de FORSK. Deux études ont été réalisées, évaluant la couverture, la qualité et la capacité du réseau : impact des systèmes d'antennes actives/avancées (AAS) en mode MIMO mono-utilisateur avec comparaison des performances entre les antennes actives en mode MIMO mono-utilisateur et multi-utilisateurs. Les résultats fournis par les antennes actives à formation de faisceau verticale se sont avérés avoir un impact positif, confirmant une augmentation de la capacité des cellules par rapport aux systèmes d'antennes traditionnels. En mode mono-utilisateur, aucune différence significative n'a été observée entre les antennes actives étudiées, contrairement à ce qui a été observé en mode multi-utilisateur, dans lequel le nombre d'émetteurs-récepteurs en plus du gain des faisceaux a confirmé l'augmentation de la capacité des cellules.

Mots clés

5G, beamforming, MaMIMO, couverture, capacité, AAS, SU-MIMO, MU-MIMO, prédictions

Abstract

The fifth generation of mobile communications, 5G, aims to meet the growing needs and greater demand of users in relation to capacity and latency, in a growth that has been exponential and that is expected to continue. This thesis aims to analyze the impact of MIMO and beamforming antennas whose technology is promising to meet the requirements on the network's performance, through predictions. This assessment was made using the radio network planning tool Atoll from FORSK. Two studies were carried out, evaluating network coverage, quality and capacity: impact of active/advanced antenna systems (AAS) in single user MIMO mode with performance comparison between active antennas in single user MIMO and multi-user MIMO mode. The results provided by the active antennas with vertical beamforming shown to have a positive impact, confirming an increase of the cell capacity compared to legacy antennas systems. In single user mode, no significant differences were observed between the active antennas under study, contrary to what was observed in multi-user mode, in which the number of transceivers in addition to the gain of the beams confirmed the increase in cell capacity.

Keywords

5G, beamforming, MaMIMO, coverage, capacity, AAS, SU-MIMO, MU-MIMO, predictions

Table of Contents

General Introduction **1**

Chapter 01: Overview and definitions

1.1 Overview **3**

1.1.1 Historical Background 4

1.1.2 5G Use Cases and Requirements 6

1.2 Motivation and Structure **9**

Chapter 02: 5G Fundamental Concepts

2.1 5G-NR Basic Concepts **12**

2.1.1 5G-NR Network Architecture 13

2.1.1.A Core Network 14

2.1.1.B Radio Access Network 20

2.1.1.C LTE Interconnection 22

2.1.2 Physical Layer 24

2.1.2.A Spectrum 27

2.1.2.B Transmission Scheme and Radio Frame Structure 29

2.1.2.C Duplex Scheme 32

2.1.3 Multi-antenna Transmission 32

2.1.3.A Beamforming 33

2.1.3.B Massive MIMO 35

2.2 Propagation Models **37**

2.3 Types of Databases **39**

Chapter 03: RF Planning tool (Atoll)

3.1 Radio Network Planning Tool **41**

3.2 Propagation Model **42**

3.3 Network Configuration Parameters **45**

3.3.1 Site Parameters 47

3.3.2 Transmitter Parameters 48

3.3.3 Cell Parameters 49

3.4 Deployment Area and Inputs 50
3.4.1 Digital Terrain Model 52
3.4.2 Clutter Classes 52
3.4.3 Clutter Heights 54

3.5 Antennas 55

3.6 Traffic Parameters 57

3.7 Predictions 57

Chapter 04: Application and results analysis

4.1 Comparison of AAS performance in SU-MIMO 61
4.1.1 Network Coverage 62
4.1.2 Network Quality 63
4.1.3 Network Capacity 64

4.1 Comparison of AAS performance in MU-MIMO 65
4.1.1 Network Coverage 65
4.1.2 Network Quality 66
4.1.3 Network Capacity 67

General Conclusion 68

References 70

List of Figures

1.1 Daily demand by category over the last 6 years 2
1.2 Evolution of cellular standards 5
1.3 Three types of Fifth Generation (5G) application scenarios 7
1.4 Enhancement of key capabilities from IMT Advanced to IMT-2020 8
2.1 High-level 5G-New Radio (NR) core network architecture 14
2.2 Control Plane and User Plane Separations (Control and User Plane Separation) 17
2.3 3GPP deployments using network slicing. 18
2.4 CN-RAN deployment options 19
2.5 5G NSA option 3x - generic operation 21
2.6 Radio Access Network architecture 22
2.7 Homogeneous (left) and heterogenous (right) deployment scenarios 22
2.8 LTE and NR network interconnection 23
2.9 Grid of SSB beams in 5G NR 27
2.10 Spectrum for current cellular systems and 5G 28
2.11 The NR numerology for wide range of frequencies and deployment types 31
2.12 Third Generation Partnership Project (3GPP) NR frame structure 32
2.13 Basic beam set #3#3#2. 35
3.1 Representative schemes of the SPM and Ray Tracing propagation models 38
3.2 Atoll working environment 41
3.3 Standard Propagation Model parameters 44
3.4 Standard Propagation Model clutter parameters 45
3.5 Deployment area (top) and site's 3D view (bottom) 51
3.6 Digital Terrain Model (DTM). 52
3.7 Clutter classes 53
3.8 Clutter heights 54
3.9 Massive MIMO antenna for 3.5GHz band with 64Tx. 56
3.10 Horizontal and vertical pattern of one of the beams 56
4.1 SS-RSRP-DL CDF by covered area. 62
4.2 Frequency polygon of the PDSCH CINR level by covered area 63
4.3 Frequency polygon of the cell capacity by covered area 64
4.4 SS-RSRP CDF by covered area 65
4.5 PDSCH CINR CDF by covered area 66

List of Tables

2.1 Core network deployment options 18
2.2 Operating bands defined by 3GPP for 5G-NR in FR1 29
2.3 Scalable OFDM numerology for 5G-NR 31
3.1 General parameters configured in Atoll 47
3.2 Site parameters configured in Atoll 47
3.3 Transmitter parameters configured in Atoll 48
3.4 Cell parameters configured in Atoll 49
3.5 Clutter classes 54
3.6 Active antennas parameters 56
3.7 Broadband service parameters 57
3.8 Terminal parameters 57
4.1 SS-RSRP-DL mean value per AAS coverage prediction 62
4.2 Numerical results of the PDSCH CINR coverage prediction. 63
4.3 Numerical results of the DL throughput coverage prediction. 64
4.4 Numerical results of the SS-RSRP coverage prediction. 66
4.5 Numerical results of the PDSCH CINR coverage prediction. 66
4.6 Numerical results of the DL throughput coverage prediction. 67

List of Acronyms

1G	First Generation
2G	Second Generation
3G	Third Generation
3GPP	Third Generation Partnership Project
4G	Fourth Generation
5G	Fifth Generation
AAS	Active Antenna Systems
AMF	Access and Mobility Management Function
API	Application Programming Interfaces
AUSF	Authentication Server Function
BBU	Baseband Unit
BS	Base Station
CA	Carrier Aggregation
CDF	Cumulative Distribution Function
CDMA	Code Division Multiple Access
CINR	Carrier-to-interference-plus-noise Ratio
CN	Core Network
CP	Cyclic Prefix
CPRI	Common Public Radio Interface
CQI	Channel Quality Indicator
CSI	Channel State Information
CUPS	Control and User Plane Separation
DC	Dual Connectivity
DL	Downlink
DTM	Digital Terrain Model
EDGE	Enhanced Data Rates for Global Evolution
eMBB	Enhanced Mobile Broadband
eNB	Evolved Radio NodeB
EPC	Evolved Packet Core
EPRE	Energy per Resource Element
EPS	Evolved Packet System
E-UTRAN	LTE Radio Access Network
FDD	Frequency Division Duplex
FR1	Frequency Range 1
FR2	Frequency Range 2
gNB	New Radio NodeB
GPRS	General Packet Radio Services
GSM	Global System for Mobile Communications
HARQ	Hybrid Automatic Repeat Request
HSS	Home Subscriber Server
IMS	IP Multimedia Subsystem
IMT	International Mobile Telecommunications
IoT	Internet of Things
IP	Internet Protocol
IS-95	Interim Standard 95

ITU-R	International Telecommunications Union, Radio Communications
LoS	Line of Sight
LTE	Long Term Evolution
LTE-A	Long Term Evolution-Advanced
MaMIMO	Massive MIMO
MCG	Master Cell Group
MCS	Modulation and Coding Scheme
MIB	Master Information Block
MIMO	Multiple Input Multiple Output
MME	Mobility Management Entity
mMTC	Massive Machine Type Communication
MU-MIMO	Multi-User MIMO
NAS	Non-Access Stratum
NEF	Network Exposure Function
NF	Network Functions
NFV	Network Function Virtualization
NR	New Radio
NRF	NF Repository Function
NSA	Non-standalone
OFDM	Orthogonal Frequency Division Multiplexing
OFDMA	Orthogonal Frequency Division Multiple Access
PBCH	Physical Broadcast Channel
PCF	Policy Control Function
PCRF	Policy and Charging Rules Function
PDCP	Packet Data Convergence Protocol
PDSCH	Physical Downlink Shared Channel
PDCCH	Physical Downlink Control Channel
PGW	Packet Gateway
PRACH	Physical Random Access Channel
PRB	Physical Resource Blocks
PSS	Primary Synchronisation Signal
PUSCH	Physical Uplink Shared Channel
PUCCH	Physical Uplink Control Channel
QAM	Quadrature Amplitude Modulation
QoS	Quality of Service
QPSK	Quadrature Phase Shift Keying
RAN	Radio Access Network
RAT	Radio Access Technology
RF	Radio Frequency
RLC	Radio Link Control
RNP	Radio Network Planning
RRC	Radio Resource Control
RRU	Remote Radio Unit
RSRP	Reference Signal Received Power
RT	Ray Tracing
Rx	Receiver
SA	Standalone

SBA	Service-Based Architecture
SCG	Secondary Cell Group
SCS	Subcarrier Spacing
SDN	Software Defined Network
SGW	Serving Gateway
SINR	Signal to Interference plus Noise Ratio
SMF	Session Management Function
SMS	Short Message Service
SPM	Standard Propagation Model
SS	Synchronisation Signal
SSB	Synchronisation Signal Block
SSS	Secondary Synchronisation Signal
SU-MIMO	Single User MIMO
TDD	Time Division Duplex
TDMA	Time Division Multiple Access
TTI	Transmission Time Interval
Tx	Transceiver
UDM	Unified Data Management
UE	User Equipment
UL	Uplink
UPF	User Plane Function
uRLLC	Ultra-reliable Low Latency Communication
UMTS	Universal Mobile Telecommunication System
VM	Virtual Machine
VoNR	Voice over New Radio

General Introduction

Over the past decades, mobile communication technology has been developing as the users demands keeps growing and new usage scenarios are discovered. The evolution of mobile communications has gone from analog voice in the 80's with the first generation of mobile communications known as 1G, to digital voice in the 90's with 2G (GSM), to mobile broadband in the beginning of the 2000 with 3G (UMTS), which enabled fast wireless internet access and left behind the voice as the main focus, to opening the way to further enhanced mobile broadband with 4G (LTE) as the main technology around 2010.

In the present days, as we face the beginning of a new decade, the 5th generation of mobile communication (5G) promises to address not only the insatiable demand for mobile broadband with multi-Gbps data rates, but also to enable new usage cases, such as massive scale communications connecting thousands of devices, sensors, cameras, providing new solutions in areas like industry, transport and logistics, agriculture and also guaranteeing ultra-reliable and low latency services with applications in the public safety area, remote surgery, communication between vehicles and so many other human life domains.

In order to be able to support all these usage scenarios the 5G technology has some key features such as beamforming, massive MIMO and the use of millimeter wave that improve the coverage and the capacity, the robustness and reliability of the communications.

The main goal of this thesis was to study the impact of advanced antenna systems (massive MIMO and beamforming) in 5G-NR networks, in order to understand the benefits of these technological techniques, by means of coverage predictions. This assessment was made through a radio network planning tool, called Atoll, which is owned by FORSK.

Chapter 01: Overview and definitions

This section provides a brief summary of the historical background and evolution of mobile communication networks, the most important aspects of the Fifth Generation (5G)-New Radio (NR) network, as well as the motivation and structure of the present thesis.

1.1 Overview

Interaction and communication are natural to humans, being one of people's basic needs. In the past, telecommunications inventions transformed the way humans interact, going beyond the reach of audio waves and visual signals. Wireless communication forms part of daily life for most people nowadays, continuously expanding in coverage, data rates and number of connected devices. Every new generation of wireless networks delivers faster speeds and work functionalities. It started with a technology capable of bringing us the first cellphones, the next one let us text for the first time, the following brought us online and the last one delivered the speeds we enjoy today. The tremendous increase in the number and variety of connected devices, the significant increase in the volume and types of user/network traffic suchlike social media apps, gaming, streaming, as well as the performance constraints of Fourth Generation (4G) technologies, have motivated industry efforts and investments to define, develop and deploy the Fifth Generation (5G) of mobile network. For the first time, in 2018, among the population covered by a mobile broadband network, there were more mobile internet users than non-users [1]. With the increasing of connected users each year, it is expected a continuous increasing throughout the following years. According to [2], audio and video streaming will become prevalent and the highest contributors to the increased traffic demand (about 79% of demand by 2020), while cloud storing services will see the most growth, which can be seen in figure 1.1.

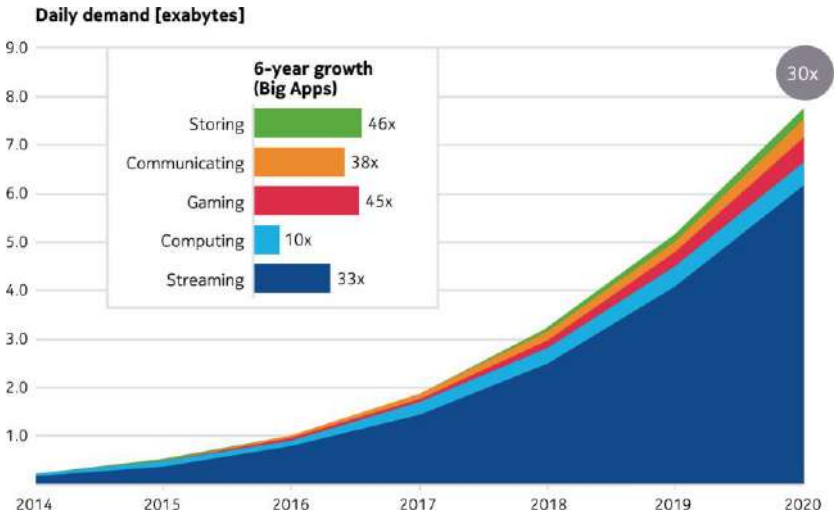


Figure 1.1: Daily demand by category over the last 6 years [2].

1.1.1 Historical Background

The First Generation (1G) cellular networks were deployed in the 1980s [3], focused on mobilizing landline telephony. The outcome networks, were circuit switched with analog voice transmission over the air. The generally decayed quality and the high sensibility to basic mobility and medium conditions represented a certain handicap of analog transmissions. Consequently, the main objective in Second Generation (2G) cellular networks was to improve voice quality. The standards have been achieved by replacing analog voice transmission with digital encryption and transmission, which greatly enhance voice communication. The improvements to the network core also made it easy for basic digital messaging services like the Short Message Service (SMS) to be introduced. The two fundamental standards of 2G networks were Global System for Mobile Communications (GSM) and Interim Standard 95 (IS-95) or cdmaOne, where the first relied mainly on Time Division Multiple Access (TDMA) and the other on Code Division Multiple Access (CDMA) as suggested by the name. This differences, alongside with variation on spectrum bands in different regions, turned out to be a major issue regarding interoperability for a long period of time.

The launch of 2G technology and the growing popularity coincided with the Internet's early years and the interest in having digital and data services of wireless and mobile device began to take shape. The evolution of the two major 2G technologies, GSM in General Packet Radio Services (GPRS) and Enhanced Data Rates for Global Evolution (EDGE), and (IS-95) into (IS-95b), has enhanced network core functionality to perform simple data transfer, facilitating interconnection with other data networks, like the Internet [4], also supporting wider bandwidths and Carrier Aggregation (CA) for the air interface [3]. After 2G became operational, the next wireless generation specifications were already being planned and debated by industry players. In parallel, the International Telecommunications Union, Radio Communications (ITU-R) developed the requirements for systems that would qualify for the International Mobile Telecommunications (IMT)-2000 classification. At this time, the Universal Mobile Telecommunication System (UMTS) was the main Third Generation (3G) mobile communication service and was one of the first cellular systems to apply for IMT-2000.

The Third Generation Partnership Project (3GPP), a standards organization that develops protocols for mobile telecommunications, upgraded the 3G into 3G Evolution. For this evolution, two Radio Access Network (RAN) approaches and an evolution of the Core Network (CN) were suggested. 3G technologies displayed that access to the Internet through a mobile phone could present users with a fine experience, and the popular use of smartphones provided by various vendors suggested a strong demand for these services. On the other hand, 3G

technologies have faced a number of challenges in adjusting the increasing demand, such as impracticable data rates at different mobility levels, degraded quality of indoor coverage, roaming difficulties (incoherent spectrum allocation between different countries) and infrastructure complexity. These and other issues have been addressed directly to a new revolution in 3G technology, namely the Long Term Evolution (LTE) from 3GPP. While the 2G and 3G have been using radio interface technologies like TDMA and Wideband-CDMA, LTE is based on Orthogonal Frequency Division Multiple Access (OFDMA) and a new architecture and CN called Evolved Packet Core (EPC) [3]. OFDMA, alongside with the Orthogonal Frequency Division Multiplexing (OFDM), is probably one of the most stunning advances in access technology, allowing subsets of subcarriers to be allocated dynamically among different users on the channel due to the trunk efficiency of multiplexing low rate, users and the ability to schedule users by frequency, which provides resistance to multi-path fading. The LTE standard offered significant capacity improvements and was designed to carry cellular networks away from circuit-switched functionality, resulting in cost reductions comparing to older generations [3]. In LTE Release 10 (known for the enhancements in capabilities of LTE to the designed LTE-Advanced) a number of technical features, such as higher order Multiple Input Multiple Output (MIMO) (configurations up to 8x8 in Downlink (DL) and 4x4 in Uplink (UL)) and CA (up to 100 MHz of total bandwidth), which increased the efficiency and performance of Release 8. Long Term Evolution-Advanced (LTE-A) prevailed as the dominant cellular access technology today and has served as the basis of the transition to 5G mobile communications. In summary, the figure below illustrates the chronological evolution of mobile communications.

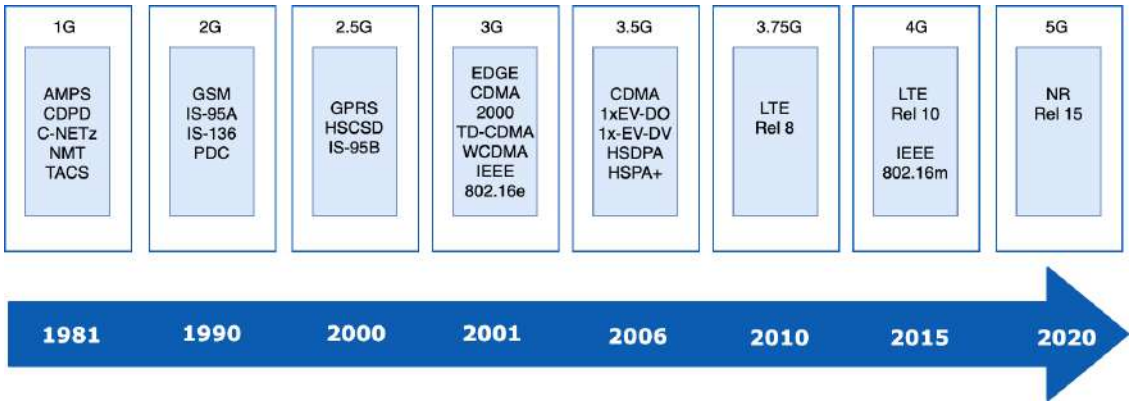


Figure 1.2: Evolution of cellular standards.

1.1.2 5G Use Cases and Requirements

5G can be considered a continued evolution of LTE. Since its launch in Release 8, LTE has experienced a number of releases. It has been optimized for more and more use cases. Eventually, the LTE standard will fulfill the IMT-2020 requirements and a 5G technology can be labeled, which is not only a new or evolved Radio Access Technology (RAT), but a well-integrated and seamlessly interoperable RATs (New RAT, LTE, Wi-Fi, etc.). Thus, 5G is more of a concept rather than a specific technology. The 3GPP view is by now certain: the first deployment of 5G will be anchored by LTE. This is called Non-standalone (NSA) 5G architecture and will be discussed in the next chapter.

Furthermore, 5G wireless access is intended to allow a networked society where data can be accessed and shared by anyone and anything, anywhere and anytime.

There are three major challenges in order to enable a fully networked society [5]:

- A massive growth in the number of connected devices.
- A massive growth in traffic volume.
- A wide range of applications with diverse requirements and characteristics.

5G wireless access requires not only new functionalities, but also substantially more spectrum and wider frequency bands to answer these challenges, specifically higher frequencies in the millimeter wave range (dozens of gigahertz). At higher frequency ranges, where networks have yet to be deployed, propagation conditions are more complex than what is commonly experienced today. Higher diffraction loss and outdoor-to-indoor losses lead to link budgets that are challenging to meet. The output power of mobile terminals, may, for regulatory reasons, be more limited at higher frequency bands. As such, these bands are best suited for dense network deployments in highly populated areas such as city centers, airports, train stations, shopping malls and indoor offices [6]. 5G seeks to provide customized coverage for a range of drastically different types of services and consumer specifications, unlike its predecessors. In accordance with the ITU-R nomenclature for international mobile communications for 2020 and be- yond (IMT-2020) [7], 5G will target three use case families with very distinct features: Enhanced Mobile Broadband (**eMBB**), Massive Machine Type Communication (**mMTC**), and Ultra-reliable Low Latency Communication (**uRLLC**). The characteristics of the three case groups, shown in the Figure 1.3, are then described [5].

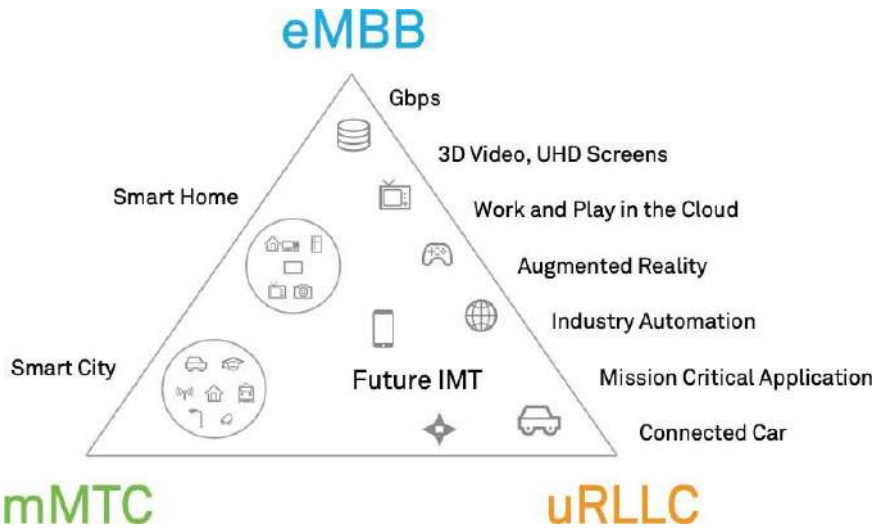


Figure 1.3: Three types of 5G application scenarios [8].

- **Enhanced Mobile Broadband (eMBB)**:

  It includes access to multimedia content, services and data and addresses human-centered connectivity. This is achieved by offering high data rates to support future multimedia services and the growing volume of traffic created by these services. The eMBB use cases includes a number of scenarios:

  - *Hotspot connectivity:* which is characterized by a high user density and extremely high data rates, and low mobility.
  - *Wide-area coverage*: where the user density and data rates are lower, but the mobility is higher.

- **Massive Machine Type Communication (mMTC)**: The growth of the Internet of Things (IoT) has resulted in a wide range of Machine Type Communication-traffic wireless devices. These services are characterized by a large number of equipment, including, for example, remote sensors, actuators and various monitoring equipment. The key requirements of these services include very low cost of equipment and very low consumption of power, which allows for very long battery lives of up to a minimum of several years.

- **Ultra-reliable Low Latency Communication (uRLLC)**: The specific features of this category of cases, which mainly focuses on machine-type communications, are stringent requirements for both latency and reliability (very low latency and extremely high

reliability). The applications under discussion include wireless monitoring of industrial production and manufacturing processes, remote medical operations, driverless vehicles and/or remotely driven vehicles, and smart grid distribution automation.

In order to meet the needs of **eMBB**, **mMTC** and **uRLLC**, the ITU-R set key performance requirements for IMT-2020. Such requirements can be seen in Figure 1.4, where there is a comparison to previous mobile generation's key capabilities IMT-advanced. The requirements include a peak data rate of 20 Gbits/s, a latency below 1ms, and the capability to support a connection density of 10^6 devices per square kilometer [7].

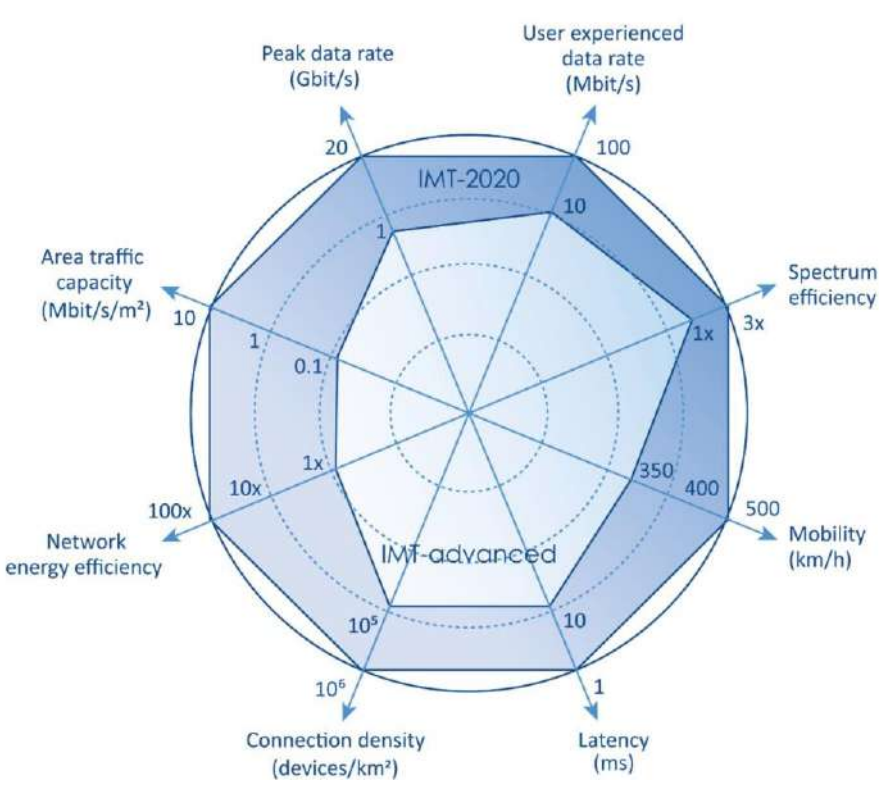


Figure 1.4: Enhancement of key capabilities from IMT-Advanced to IMT-2020 [7].

At this stage, based on the 3GPP release 15, 5G-NR network is focused on eMBB service, so the target of 5G-NR at this time is to meet the eMBB requirements.

1.2 Motivation and Structure

There are an increasing number of devices connected to the mobile network, requiring connections with higher performance and low latency. According to [9], there are now 6 billion mobile broadband subscriptions, and this number is expected to reach 8.3 billion mobile broadband subscriptions by 2024. This represents 95% of all the mobile subscriptions. Consequently, to meet the new requirements, a new radio is also required, named 5G-NR, arriving with capabilities that enable new technologies to be built and meet today's demand for services.

The main objective of this thesis is to assess the impact of technologies such as massive MIMO and beamforming in a 5G network, by means of coverage predictions. The study was based on the Atoll radio network planning tool, provided by FORSK, a well-known US telecommunications company. The simulation and scenarios are made for city of Oran, a large city in the west of Algeria.

In terms of structure and content, this study is divided into four chapters, in the first chapter, was provided a brief description of the evolution of mobile communication over time, as well as the motivations behind the need to improve communication networks, addressed to the new digital revolution. The 5G use cases and requirements are also part of this chapter, which ends with the motivation and structure of the present thesis.

The 5G-NR theoretical background is presented in the second chapter. Basic concepts about the network architecture, physical layer, multi-antenna transmission and propagation models are covered in this chapter. In this early stage of 5G-NR, most of the deployment will be supported by the LTE core network, in which a brief description of this interconnection is given. The physical layer, as the backbone of any network, is described through channels, spectrum, synchronization signals and transmission schemes. It is also addressed the theory behind the technologies in focus on this thesis: massive MIMO and beamforming. The chapter ends with the differences between the propagation models and the type of database that serve as a basis for these propagation models.

Chapter 3 is named RF planning tool (Atoll), since it is in this chapter that is explored all the details regarding the radio network propagation tool. A brief overview of the radio network planning tool used is given, and the propagation model chosen to evaluate the predictions, which is empirical and based on extensive measurement campaigns and experiments. Subsequently, the majority of the inputs, such as network configurations or geographic data, necessary for the *Atoll* predictions were presented. The network configuration is started by the geographical introduction

of the site and its parameters. Some parameters common to all predictions are presented, followed by the transmitter parameters. Lastly, the cell parameters that characterize the RF channel, as well as a short description of each. The city of Oran, in west Algeria, was chosen as the reference scenario for this study, as it is considered as urban and Sub-urban area, where most of the first 5G networks are implemented. A screenshot of the different terrain database inputs is presented, such as DTM, clutter classes and clutter heights. Furthermore, the types of antennas that will be part of the predictions are presented: active antennas composed of 3 different models, which differ mainly in the number of transceivers. All antennas under study operate with the same frequency, bandwidth, maximum power and horizontal radiation width. Last but not least, the four different types of predictions are introduced: network coverage, network quality, service areas and network capacity, accompanied by a brief description. The user profile and the type of service associated with the predictions is also reported.

Chapter 4 presents the results obtained from the forecasts that were evaluated in this thesis and the respective analysis. Two different analyses were made and are organized in two different sections.

Chapter 02: 5G Fundamental Concepts

This chapter presents some basic concepts and key characteristics of a 5G-NR network, the 5G millimeter wave communications and multi-antenna transmission particularly beamforming and Massive MIMO concepts.

2.1 5G-NR Basic Concepts

5G-NR is the 5th mobile networks generation, a major development of today's 4G LTE networks. 5G is built to respond to today's society's very big rising data and networking, the Internet of things with billions of devices connected and the inventions of tomorrow. 5G will initially work with existing 4G networks before evolving into fully independent networks in subsequent releases and extensions of coverage. Besides the fast throughput rates and great capacity, a very important advantage of 5G is the low latency (i.e., fast response time), enabling a truly real-time connected world. On top of that, a fundamental aspect of global mobile services is the possibility of operating a radio access technology in different frequency bands, where NR does not assume any specific band. The objective is to aggregate different bands of spectrum from sub 1 GHz to millimeter waves in order to provide the best combination of coverage, capacity, and user data rates. NR can be deployed in different frequency bands, which were established by 3GPP on the Release 15. Such bands were divided into two frequency ranges mostly due to different Radio Frequency (RF) requirements (e.g., maximum transmission power):

- **Frequency Range 1 (FR1)** that includes all existing and new bands below 6 GHz.
- **Frequency Range 2 (FR2)** that includes new bands in the range of 24.25 - 52.6 GHz.

These frequency ranges may be expanded or supplemented with new ranges in future 3GPP releases.

In terms of Modulation and Coding Scheme (MCS), NR supports Quadrature Phase Shift Keying (QPSK), 16 Quadrature Amplitude Modulation (QAM), 64 QAM and 256 QAM modulation formats for both uplink and downlink, as in LTE. Since NR can reach a wide range of applications, it is potentially possible to expand the number of approved modulations. Lower MCS (under 64-QAM) are more robust (i.e., least chance of losing data) and tolerant to higher values of interference although at a lower transmission throughput, while higher MCS orders (64-QAM and above) have much higher transmission throughput, but are less robust (i.e., greatest chance data can be lost) and more sensitive to noise and interference [10]. MCS also defines coding rate, varying from 1/5 to 8/9 [11]. A high code rate means information content is high and coding overhead is low. However, the fewer bits used for coding redundancy, the less error protection is provided [12]. Despite that, the real ratio of useful bits to total transmitted bits depend on radio link quality, that is reported by the User Equipment (UE) to the Base Station (BS) through Channel Quality Indicator (CQI).

The extensive research on multiple access has shown that OFDMA is able to provide both downlink and uplink with fairly high system throughput for eMBB [13], hence being at least mandatory for NR, not excluding other non-orthogonal multiple access schemes that can be complementary in some specific use cases, for instance, IoT, with the capability to support multiple users within one resource block, potentially supporting massive connectivity for billions of smart devices [14].

The waveform that has been adopted for the 5G-NR is based on OFDM, a multi-carrier waveform, but with updates to that used with LTE. The 3GPP agreed in favor of Cyclic Prefix (CP)-OFDM for both uplink and downlink communications, taking into account overall performance, network specifications and the need of a single waveform. CP-OFDM ranks best on the performance indicators that matter most compatibility with multi-antenna technologies, high spectral efficiency, and low implementation complexity [15].

With the new range of frequencies required by 5G-NR, especially in the highest frequencies, propagation conditions are more challenging due to the very fast attenuation of the signal. Beamforming and Massive MIMO (MaMIMO) can be used as a tool to improve link budgets specially at these higher frequencies. These two terms are sometimes used interchangeably, being beamforming a subset of MaMIMO.

In a nutshell, beamforming is the ability to adapt the radiation pattern of the antenna array to a particular scenario [16], rather than spreading the signal from the transmitting antenna in all directions, as it would usually be. The result is a more direct connection, which is faster and more reliable.

As for the Massive MIMO, Massive simply refers to the large number of antennas in the base station antenna array [16]. MIMO (Multiple-Input Multiple-Output) technology, as the name suggests, is a wire- less technology that uses multiple transmitters and receivers to transfer more data at the same time. It has been more widely used with LTE, and the concept has proven to improve significantly [17].

2.1.1 5G-NR Network Architecture

Simultaneously to the work on the 3GPP NR radio-access technologies, the overall system architectures were reviewed, namely the Radio-Access Network (RAN) and the Core Network (CN) and respective functionalities.

2.1.1.A Core Network

The mobile core network is responsible for functions such as session management, mobility, authentication, and security. The point-to-point architecture used in legacy networks contained a large number of unique interfaces between functional elements, each connected to multiple adjacent elements, making it difficult to change a deployed architecture or to add a new function due to all the reconfiguration needed. However, with the transition to cloud infrastructure and the need for greater service agility able to adapt to fast-changing demand, the service-based architecture is more suitable and attractive. In this way, the 5G core network relies on the EPC but with three additional enhancement areas compared to the EPC: Service-Based Architecture (SBA), Network Slicing support, and Control and User Plane Separation (CUPS) [18].

The goal of the Service-Based Architecture (SBA) is to migrate from telecom-style protocol interfaces to web-based Application Programming Interfaces (API), allowing services to register themselves and subscribe to other services. This enables a more flexible development of new services, as it becomes possible to connect to other components without introducing specific new interfaces. Figure 2.1 presents the non-roaming architecture specified in 3GPP technical specification 23.501 [19]. As [20] states, in this high-level architecture representation, the control-plane functions, shown above the dotted line, connect to each other through service-based interfaces. The Access and Mobility Management Function (AMF) and Session Management Function (SMF) connect to user-plane nodes via N1, N2 and N4 interfaces to manage subscriber attachment, sessions and mobility. The N2 and N3 interfaces are determined by how the 5G radio presents itself to the core, and therefore, are dependent on the 5G RAN architecture [20].

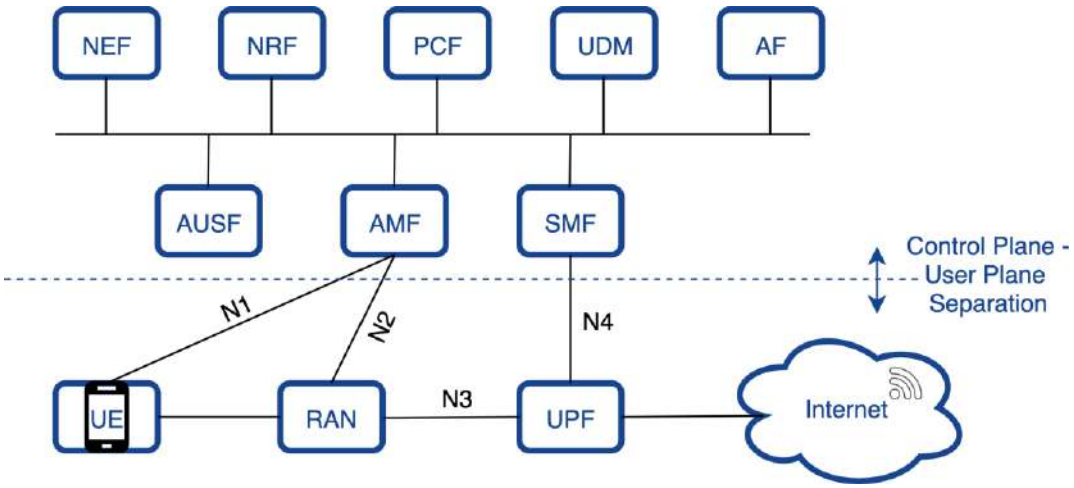


Figure 2.1: High-level 5G-NR core network architecture (adapted from [21]).

The main components of the 5G core is divided by user-plane functions and control-plane functions and are listed below [19][20]:

- **Access and Mobility Management Function (AMF):** this control-plane function is in charge of control signaling between the core network and the device (referred to as Non-Access Stratum (NAS)), security for user data, authentication and idle-state mobility. Corresponds to the mobility management functions of the EPC Mobility Management Entity (MME).
- **Session Management Function (SMF):** also part of the control-plane function, it supports the session management (session establishment, modification and release), Internet Protocol (IP) ad- dress allocation for the device (also known as UE) and control of policy enforcement. Corresponds to the session management functions of the EPC MME and Packet Gateway (PGW).
- **User Plane Function (UPF):** is a gateway between the RAN and external networks such as Internet. Supports packet routing and forwarding, packet inspection, Quality of Service (QoS) handling, traffic measurement, and is an anchor point for intra-RAT mobility. Corresponds to the user plane functions of the EPC PGW and Serving Gateway (SGW).
- **Policy Control Function (PCF):** responsible for policy rules incorporating network slicing, roaming and mobility management. Corresponds to the EPC Policy and Charging Rules Function (PCRF).
- **Unified Data Management (UDM):** generation of authentication and key agreement credentials, user identification handling, access authorization, subscription management. Similar to Home Subscriber Server (HSS) in EPC, but will be used for both fixed and mobile access.
- **Authentication Server Function (AUSF):** as the name implies, this is an authentication server. Correspond to a part of the HSS from EPC.
- **NF Repository Function (NRF):** this new feature allows registration and discovery functionality in order to discover and interact with Network Functions (NFs) through APIs.
- **Network Exposure Function (NEF):** an API gateway that permits the control, provision and enforcement of application policies for applications within the network operators by external users, such as enterprises or affiliate operators.

The 5G core architecture is programmed to be cloud-native in terms of making use of Network Function Virtualization (NFV) and Software Defined Network (SDN) techniques. By enabling virtualization in the core network, service providers can significantly decrease operational expenditure and capital expenditure, while accelerating the delivery of customized services.

For NFV, the process involves decoupling software from hardware in a way of performing network functions like firewall and encryption on Virtual Machine (VM). Such VMs operate on network nodes that administrators can use to set up a network-connected device service chain. Whenever a customer requests for a network upgrade or installation, the service provider can boot up a VM to solve the request using a mix of switches, storages and servers, resulting in a high-performance network with great scalability and elasticity at a reduced cost compared to networks built from traditional hardware networking equipment.

As mentioned previously, the SDN can virtualize the core network as well, enabling networks to be centrally controlled through software applications that use open APIs. SDN basic principle is separation of network control functions, known as control plane, from data traffic forwarding, known as user plane. This principle is called CUPS[22] and its concept is briefly summarized in figure 2.2. With the current pressing for reducing network costs and the increasing cellular network requirements, the use of CUPS concept when standardizing the architecture for any new telecommunication network seems an absolute necessity. Control plane capabilities are executed by a SDN controller, an application that manages flow control and addresses varied needs to update the network automatically. The SDN controller platform typically runs on a server and uses protocols to tell switches where to send packets [23].

CUPS principle was introduced in 4G EPC, where the SGW and PGW functions were split into a control and data component: from Serving Gateway (SGW) to SGW-C and SGW-U and from Packet Gateway (PGW) to PGW-C and PGW-U. Later the 4G EPC components have been reorganized into the service-oriented functions described previously.

CUPS reduce application service latency by choosing user plane nodes which are closer to the RAN or more suitable for the intended UE usage type, without increasing the number of control plane nodes. This mechanism is very much efficient for high-bandwidth applications (e.g., video streaming). Since the main user plane node is situated near the end user, the operator doesn't have to transmit user data all the way to the central hub, thus saving time and money. These plane functions scale independently. By way of example, higher demand for data traffic is supported by adding additional user plane nodes without increasing control plane nodes in the network.

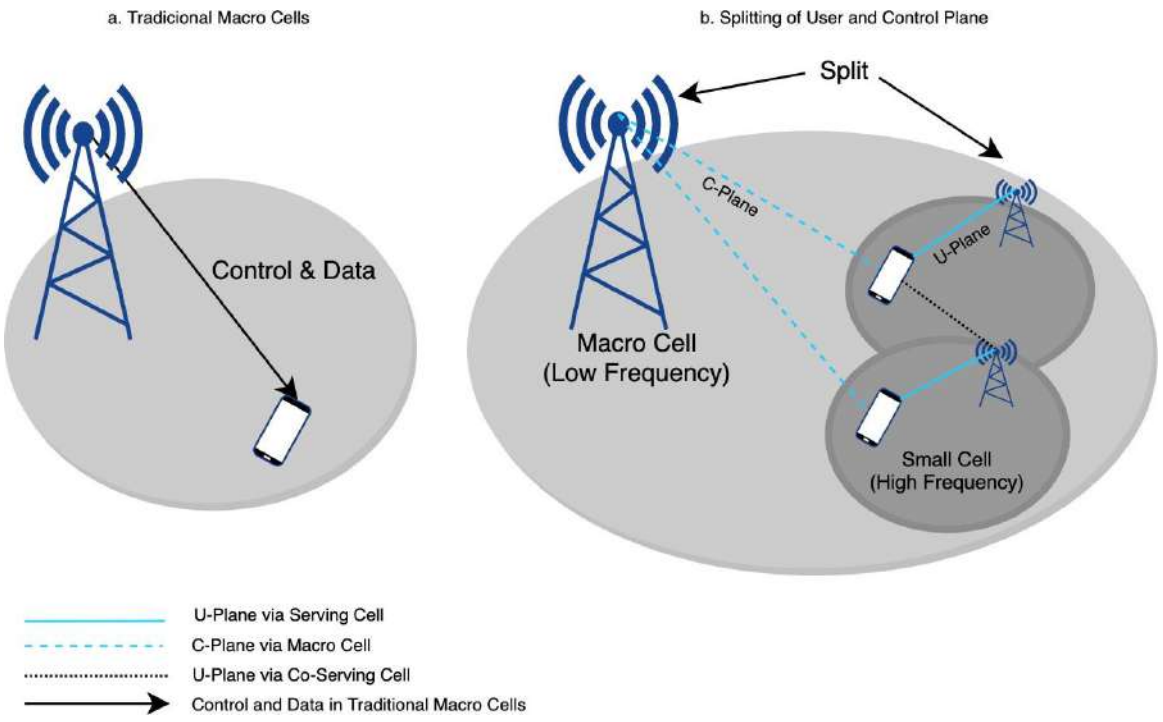


Figure 2.2: Control Plane and User Plane Separations (CUPS).

Despite of NFV and SDN not being dependent on each other, their complementarity allows a programmable network infrastructure, agile and cost-efficient. Both features have led to the development of network slicing and service function chaining.

Network slicing is another core enabling technology, which leverages both the principles of NFV and SDN. With network slicing, network operators can divide a single, physical network into various virtual networks, with each slice representing an independent, virtualized end-to-end network, with functionality specific to the service or customer. This ability to support several customer and service types with individual performance requirements (e.g., transmission rate, latency, throughput) is probably the most important commercial driver for 5G. Network slicing consists of two groups [24]. One is a dedicated network slice and the other is the network slices sharing common control planes Network Functions (NF). Global network functions across multiple slices, e.g., UE subscription repository function. An example of network slice with shared and dedicated resources combined is shown in figure 2.3, under the architecture adopted in 3GPP Release 15. This illustration gives an outlook of the wide range of possible configurations for different network slices in reference to different use cases required.

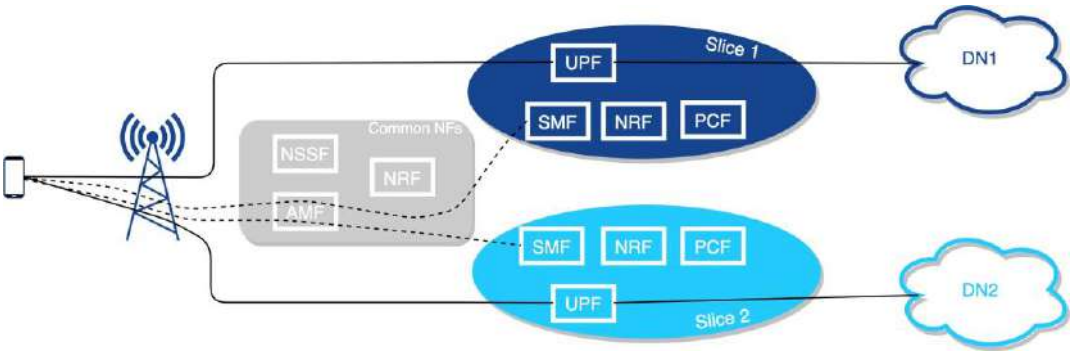


Figure 2.3: 3GPP deployments using network slicing (adapted from [25]).

The concepts above focused on the new 5G core network and it was developed in parallel to the NR radio access. For CN-RAN deployment, 3GPP has fixed several options [26], table 2.1.

The options using Dual Connectivity (DC) are categorized under the term Non-standalone (NSA), to specify that 5G-NR and LTE are used simultaneously to provide radio access. Standalone (SA) is the option where only one radio access technology is in use.

Type	Option	Core Network	RAN	Comments
Standalone	1	EPC	eNB	Native LTE
Standalone	2	5GC	gNB	Pref. SA option
Standalone	5	5GC	NG-eNB	
Non-standalone	3/3a/3x	EPC	eNB, SgNB	LTE as an anchor
	4/4a	5GC	gNB, NG-eNB	gNB as anchor
Non-standalone	7/7a/7x	5GC	NG-eNB, gNB	LTE as an anchor

Table 2.1: Core network deployment options [10].

As mentioned in section 1.1.2, the first rollout of 5G networks will be anchored by LTE (NSA deployments). NSA architecture allows the mobile network operators to leverage their current networks, saving investments, and supplying their customers with high data speed connectivity. SA NR deployment is expected to arrive later, beyond 2020, when availability of NR capable devices and their market uptake, new use cases (e.g., mMTC, uRLLC) start to gain momentum and NR spectrum gets an even wider access.

As evidenced in table 2.1, option 3 is the 5G technology candidate submitted by 3GPP comprising both LTE and NR and therefore it is the option that this document will focus on.

Non-standalone option 3 is where radio access network is composed of a LTE base station (Evolved Radio NodeB (eNB)s) as the master node and 5G base station (New Radio NodeB (gNB)s) as the secondary node. They are connected by the X2-interface. The radio access

network is connected to EPC by the legacy S1-interfaces. In this scenario, the NR gNB is seen by the EPC as a secondary RAT within LTE Radio Access Network (E-UTRAN). LTE is used as the control plane anchor for NR, and both LTE and NR are used for user data traffic (user plane). The NR gNB may have a user plane connection over S1 to SGW, but no control plane connection over S1 to MME, so the data routing will vary depending where to split the user plane between LTE and 5G. Taking into account these variants, option 3 is divided into: **option 3**, **option 3a**, **option 3x** illustrated in figure 2.4 [26] and detailed below [21].

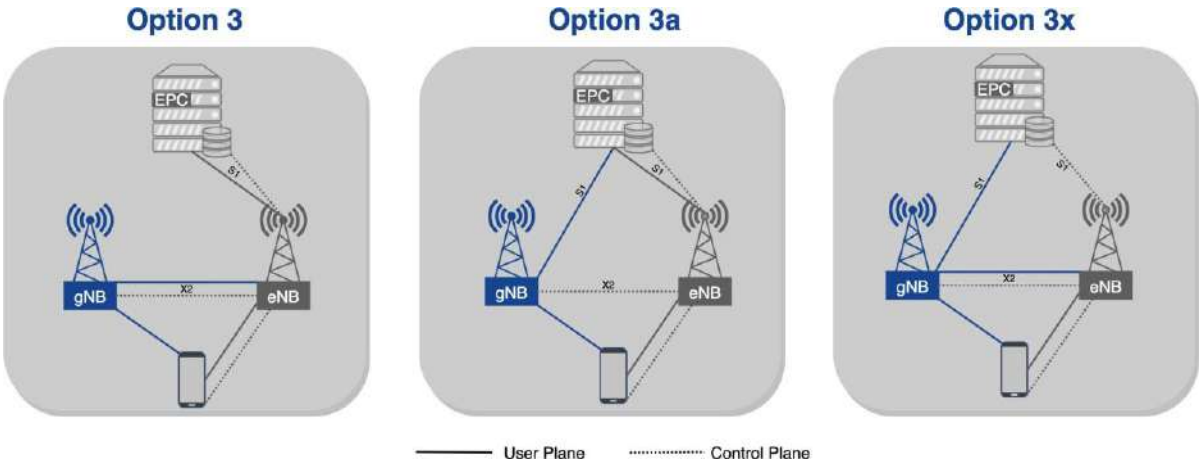


Figure 2.4: CN-RAN deployment options.

- **Option 3**: with user data split in the LTE eNB. The traffic flow is converged at eNB Packet Data Convergence Protocol (PDCP) layer and distributed from the eNB to the gNB over the X2 interface. This permits the transmission of a single service with bearer split, called Master Cell Group (MCG) split bearer, from both the gNB and eNB and respectively received from both sides in uplink. Control plane relies on Evolved Packet System (EPS) LTE S1-MME interface and LTE Radio Resource Control (RRC). In this scenario, eNB nodes will carry a large amount of traffic and related computer load and therefore eNB hardware upgrade is required, such as the backhaul to the core network and between the nodes.

- **Option 3a**: with user data split in the EPC. gNB also has S1-U interface to EPC but there is only control plane traffic in the X2 interface, turning the demand for this late interface easy to meet. This means no sharing of data load between the nodes, and the different service bearers are carried either by an LTE eNB or a NR gNB. For this reason, new services that needs higher throughputs or ultra-low latency can be handled by NR. Low data rate services like Voice over New Radio (VoNR), are managed by the eNB while data traffic is managed by the gNB.

- **Option 3x**: with data split in the 5G gNB. It is a combination between option 3 and 3a. In this configuration, gNB has S1-U interface to EPC. User data traffic will flow directly to the 5G gNB part of the base station and can be divided with the 4G eNB over the X2 interface, called the Secondary Cell Group (SCG) split bearer. In this architecture, most of the traffic is carried with high performance by the 5G gNB. By using 4G as the anchor point of the control plane, the service enhancements provided by the 5G gNB and the small impact on the existing network, Option 3x has become the mainstream choice for NSA deployments [27][26].

Introducing 5G with NSA option 3X, reutilizing an already deployed LTE core, is the fastest, easiest and cheapest way for operators to provide immediate 5G services such as high end-user throughput and low latency data connections. A generic operation of this option is shown in figure 2.5. While downloading or streaming packets, if the UE enters the gNB area, the bearer path once connected to the eNB is switched to the gNB and the device is served of additional user plane capacity. In case of an incoming voice call, the IP Multimedia Subsystem (IMS) architecture framework enables the delivery of multimedia services over any access network, for example the previously mentioned VoNR, and the voice packets run through a different bearer over the eNB, while the service is managed by the eNB.

2.1.1.B Radio Access Network

The radio-access network can have two different nodes attached to the core network: eNBs for LTE radio access and gNBs for NR radio access. Each of these complex base stations are composed of a Baseband Unit (BBU) and a Remote Radio Unit (RRU). The BBU is in charge of baseband signal processing, coding, encryption, resource scheduling, and interfacing with the core network and other eNBs/gNBs [29], namely the Common Public Radio Interface (CPRI) interface for communication with RRUs, the S1 interface for communication between the eNB/gNB and an MME/SGW and X2 interface between base stations. On the other side, the RRU is the RF circuitry in a small module of the base station that performs all the RF functionality such as up-conversion and down-conversion between the baseband signal and the carrier frequency, signal amplification, and other RF functions. It can also pro- vide advanced monitoring and control features that enable operators to optimize performance remotely. The RRUs are located on the tower and linked via fiber optic cable to the BBU (generally positioned at tower base) through the CPRI interface. Figure 2.6 illustrates this network architecture.

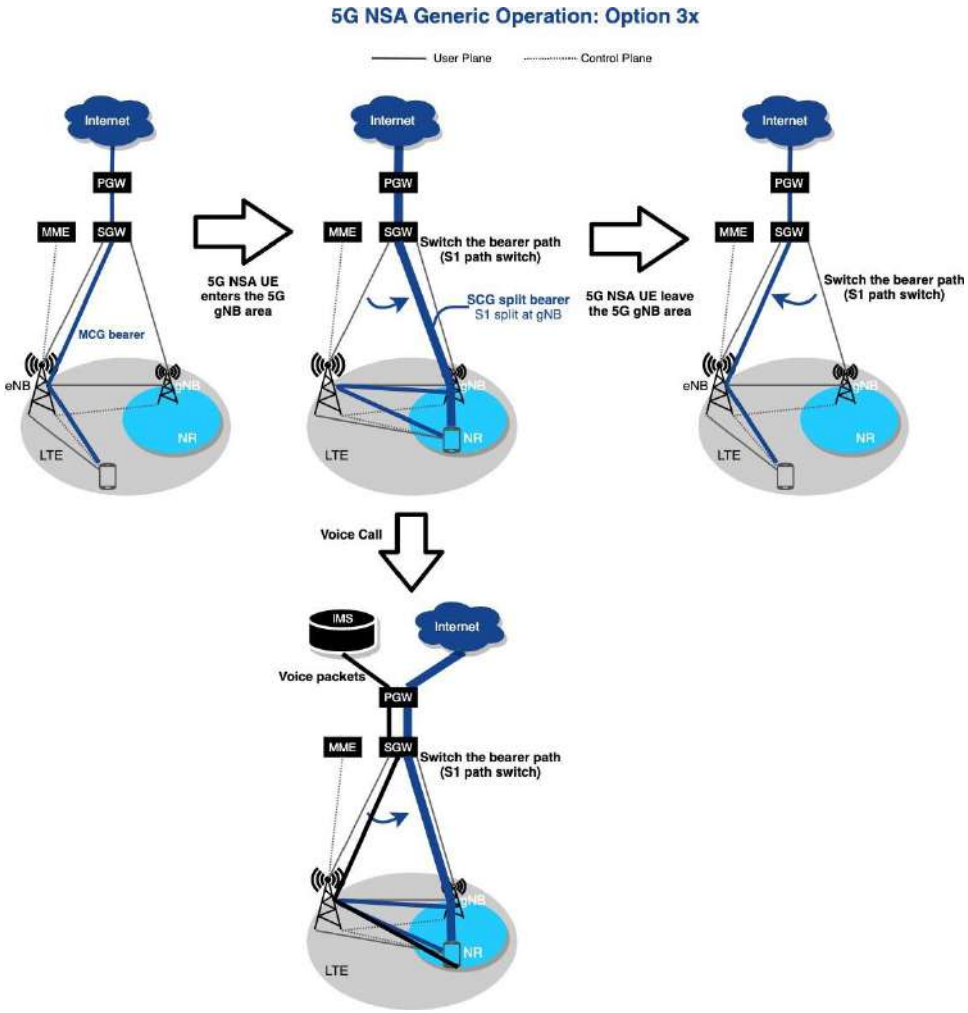


Figure 2.5: 5G NSA option 3x - generic operation (adapted from [28]).

Dual connectivity is of great importance between LTE and NR since it is the basis for non-standalone operation using option 3 as shown in figure 2.4. This feature has been standardized in LTE network and now adopted for the NR NSA configuration. Dual connectivity implies that a UE is connected to two cells at the same time, thus separately receiving LTE and 5G signals then aggregating the streams. The LTE-based master cell handles control plane and (potentially) user plane signaling, while the NR-based secondary cell handles user plane only, essentially increasing the data rates [18].

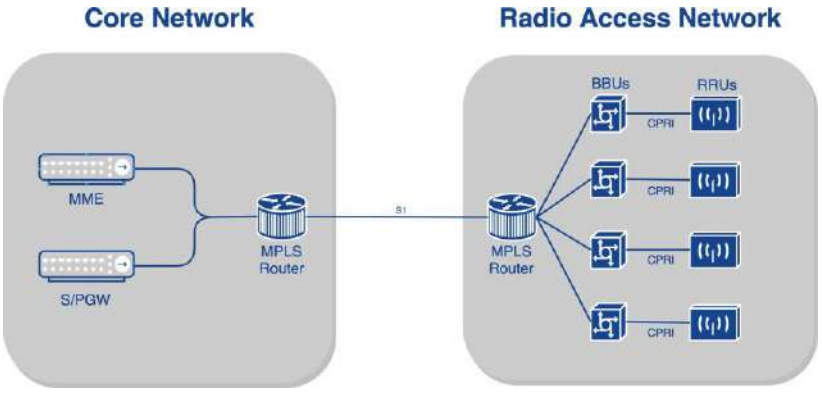


Figure 2.6: Radio Access Network architecture (adapted from [29]).

These cells in terms of cell layout can be deployed in two different scenarios, shown in figure 2.7. In the homogeneous scenario, LTE and NR cells are overlaid and co-located, providing similar coverage. In this context, both cells are either macro or small cells [11]. On the other hand, the heterogenous scenario has overlaid cells but not mandatorily co-located. The different sizes of the cells support the main objective of this next generation, a service-oriented network, as the macrocells are used as anchor points and provide wide-area coverage while the smallcell provide high-throughput small coverage within macrocell coverage [11].

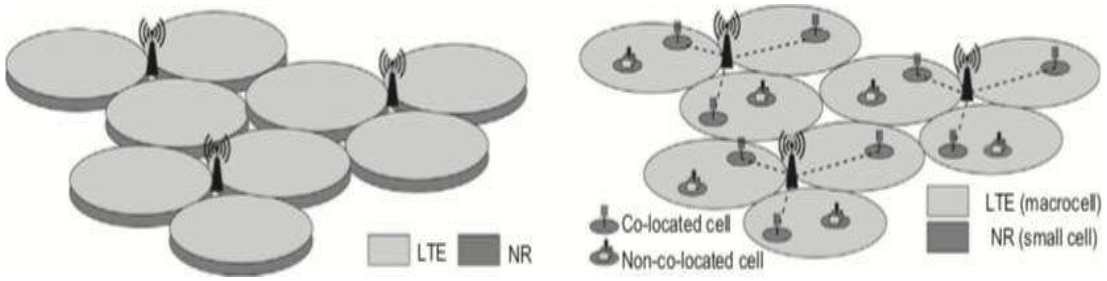


Figure 2.7: Homogeneous (left) and heterogenous (right) deployment scenarios [11].

2.1.1.C LTE Interconnection

Interworking between NR and LTE is a reality for the early deployments of the new generation of mobile communications. In later releases, a full NR based core and radio access network will be implemented. Dual connectivity, as stated previously in section 2.1.1.B, plays an important role for NSA option 3, providing high user data rates to the end user by allowing aggregation of the throughput of the NR and LTE carriers, yet anchoring in the control plane support by 4G eNB. The LTE anchor layer provides control signaling to allow the UE to set up a NR bearer when in dual connectivity mode and thus connect to the gNB [30]. A device can connect simultaneously to several nodes within the RAN, either a LTE master node or a gNB secondary node. The possibility for an LTE-compatible NR numerology based on 15 kHz subcarrier

spacing, enabling identical time/frequency resource grids for NR and LTE, is one of the fundamental tools for such coexistence [18] and will be explained in the forthcoming section 2.1.2.B.

The mainstream option for early deployment defined by 3GPP [26] has both eNB and gNB relied on the LTE core, named EPC. The modules from the 5G network have already been explained and its functions are related to the LTE EPC, described below:

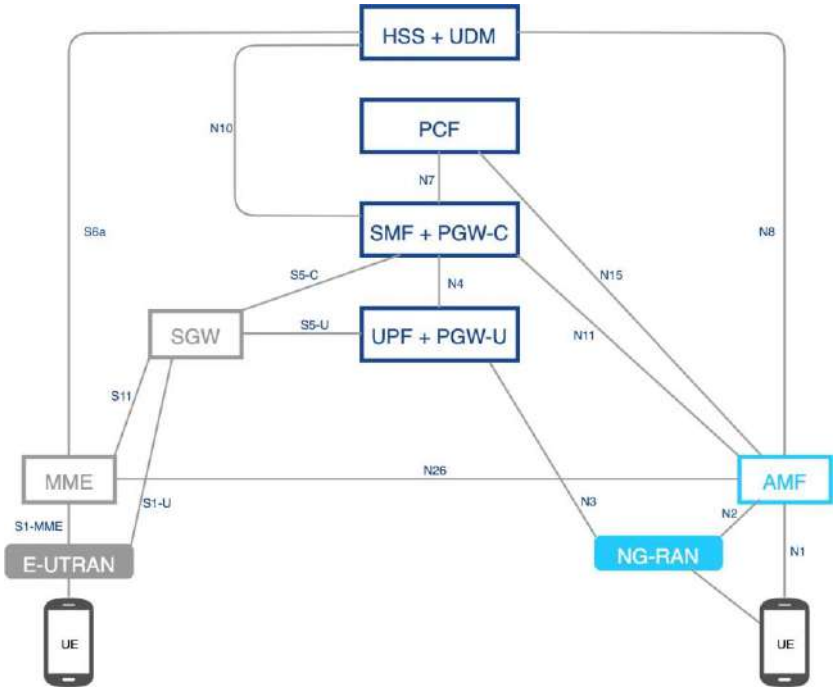


Figure 2.8: LTE and NR network interconnection (adapted from [19]).

- **Mobility Management Entity (MME)**: Control plane element that manages network access and mobility manages how UEs interact with the network. Communicates with the HSS for user authentication and subscriber profile downloads. Communicates with the eNB and SGW for session control and bearer setup.
- **Serving Gateway (SGW)**: Important entity on the user plane, serving as the local mobility anchor for UE. Supports user plane mobility by IP routing and forwarding functions and maintains data paths between eNBs and the PGW.
- **Packet Data Network Gateway (PGW)**: Serves as the IP access gateway, providing the UE with an IP address and connecting to the packet data network. Facilitates flow-based charging providing records to external billing/charging systems, thus supporting policy decisions coming from the PCRF.

- **Policy and Charging Rules Function (PCRF)**: as a policy management entity, it determines how users are charged and which services are allowed to access. Manages the policies for user traffic e.g., priorities, copyrights, etc. Pairs with PGW, guaranteeing a righteous QoS.
- **Home Subscriber Server (HSS)**: stores permanent subscription details for each subscriber in the network, including the authentication key. Also stores temporary mobility and service data for every subscriber and their MME address in database.

2.1.2 Physical Layer

The radio protocol architecture for NR is divided and ordered from the lowest layer to the highest: physical (PHY) layer, medium access control (MAC) layer, radio link control (RLC) layer, packet data convergence protocol (PDCP) layer and service data adaption protocol (SDAP) layer.

The physical layer is the backbone of 5G-NR, as with any wireless technology. A wide range of frequencies (from sub-1 GHz to 100 GHz) and multiple cell deployment options (Macro, Micro and Pico cells) must be supported by the NR physical layer. 3GPP is developing a flexible NR physical layer to successfully meet the challenging requirements of ITU-R, in order to be optimized with an accurate understanding of radio wave propagation. Also known as Layer 1, the physical layer is responsible for the step-by-step process of converting bits into radio waves. Channel coding is one of the first processing steps, regarding protection and encryption of the information. Two capacity-achieving channel coding schemes of low-density parity-check (LDPC) codes and polar codes have been adopted for 5G where the former is for user data and the latter is for control information [31]. Thereafter, modulation takes place, where bits are converted into modulation symbols. Modulation schemes supported are QPSK, 16 QAM, 64 QAM and 256 QAM, as stated previously in section 2.1, where each modulation symbol corresponds to 2, 4, 6 or 8 bits respectively. After mapping the modulated symbols onto parallel streams, they are multiplied by a different subcarrier frequency, equally spaced as they achieve orthogonality between subcarriers, defining a digital multi-carrier scheme called OFDM. Finally the digital OFDM signal is converted to an analogue signal and up-converted to the selected carrier frequency (e.g., prime 3.5 GHz [32]).

There are three different types of channels in the radio channel architecture: logical channels,

transport channels and physical channels, assigned to different entities of the radio protocol stack with distinguished functionalities. Logical channels describe the type of information it carries (e.g., system information, signaling or data), transport channels describes how and with what characteristics the in- formation is transmitted (e.g., format), and the physical channels provide the transmission media through which the information is actually transmitted. A distinction can be made between physical channel, on which they carry data and information from higher layers incl. control, scheduling and user payload; and physical signals, generated in Layer 1 (hence does not carry information originating from higher layers) and used for system synchronization, cell identification and radio channel estimation [33].

The diverse physical channels defined for NR are specified for uplink and downlink [34][5][18]:

- **Physical Downlink Shared Channel (PDSCH)**: it is the main downlink radio resource in a cell. Carries data and/or higher layer signaling (e.g., paging information, RRC signaling and system information blocks) and can be allocated to different UEs on a dynamic scheduled time basis.
- **Physical Downlink Control Channel (PDCCH)**: it is used for downlink control information such as assignment and scheduling of radio resources on downlink and uplink transmission.
- **Physical Broadcast Channel (PBCH)**: it is used for broadcasting system information (specifically the Master Information Block (MIB)) required by the device to access the network.
- **Physical Uplink Shared Channel (PUSCH):** is the uplink counterpart to the PDSCH.
- **Physical Uplink Control Channel (PUCCH):** an information uplink control channel, used by the UE to send channel quality and state indicators, uplink scheduling requests and Hybrid Automatic Repeat Request (HARQ) feedback acknowledgments.
- **Physical Random-Access Channel (PRACH)**: used by the UE to request connection setup referred to as random access.

Both downlink and uplink transmission between base station and UE in the physical layer are explained below.

Concerning the downlink transmission, the procedure starts by the monitoring of the PDCCH by the UE until detecting a valid PDCCH. Once identified, the unit of data (i.e., transport block)

is scheduled by the base station and sent to the UE over the PDSCH. Subsequently, it is the UE turn to send back a HARQ as a feedback whether the data was decoded successfully or not. If not, a retransmission is scheduled [5].

Regarding the uplink transmission, the procedure starts by the scheduling request of physical time- frequency resources by the UE to the base station, via the PUCCH. The authorization is sent from the base station over the PDCCH to the UE, and consequently the data is transmitted over the PUSCH. The same HARQ error controlling method is used, though this time by the base station upon receiving uplink data, and in case of an erroneous decoding, a retransmission is scheduled.

The previously mentioned set of time-frequency resources represent the either physical channels or physical signals, the latter used for synchronization and measurements, for instance, channel state information, demodulation and channel estimation [5]. These synchronization signals are transmitted twice per radio frame (10ms) [35]. Some of these physical signals, particularly Primary Synchronization Signal (PSS) and Secondary Synchronization Signal (SSS), are used for cell search and identification. Cell search is the process by which an UE gathers the synchronization of time and frequency with a cell and decodes the physical cell identity, named Cell ID, obtained by combining both sector ID and group ID from PSS and SSS, respectively. NR supports up to 1008 physical cell identities, twice as many as that of LTE [36].

These two synchronization signals (PSS and SSS) and the PBCH together form an Synchronization Signal (SS)/PBCH block, also known as Synchronization Signal Block (SSB), that is transmitted in four OFDM symbols across 240 subcarriers in the frequency domain and in predefined bursts across the time domain, whose periodicity in terms of time slots relies on which subcarrier spacing numerology is set. The PBCH carries the MIB, the most important information block (which provides system bandwidth, antenna configuration parameters, system frame number), and its own demodulation reference signal (DMRS). In case of beamforming, each beam transmits the same PSS and SSS, same MIB, excepting the demodulation reference signal (DMRS) that is different and allows the identification of each beam. All the SSB transmitted, regardless of number of beams, are arranged in periodical burst series within one half radio frame (5ms). This scheme is illustrated in figure 2.9.

As the SSB is repeated for each beam during the sweeping, in respect to the UE, a search and measure is made for the beams, identifying which beam was received the best, and providing

corresponding feedback for the gNB. The metrics measured are SS-Reference Signal Received Power (RSRP), SS- RSRQ, and SS-Signal to Interference plus Noise Ratio (SINR) for each beam.

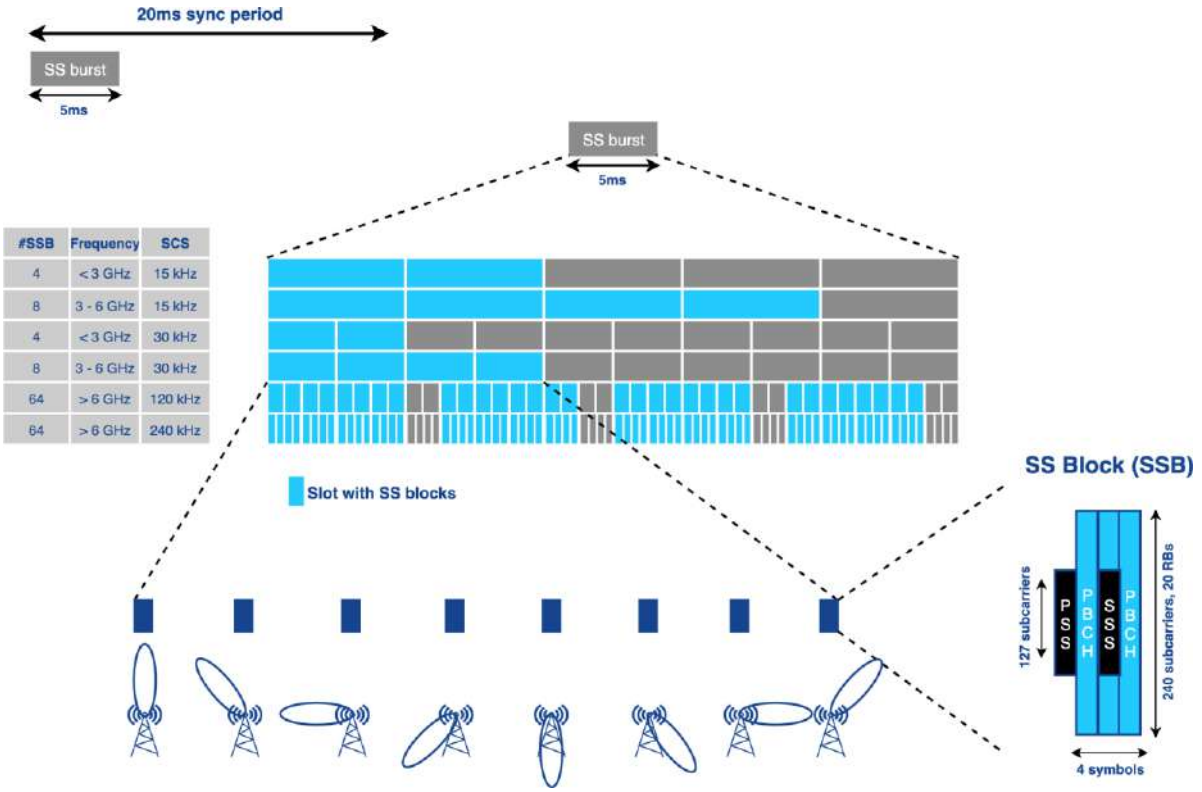


Figure 2.9: Grid of SSB beams in 5G NR (adapted from [37]).

2.1.2.A Spectrum

Spectrum availability can differ around the globe between regions and countries, in terms of bands, amounts and timing. The available spectrum has a huge impact on the definition of a network's maxi- mum capacity and coverage. As mentioned in section 1.1.2, 5G wireless access requires not only new functionalities, but also substantially more spectrum and wider frequency bands to answer these challenges, specifically higher frequencies in the millimeter wave range (dozens of gigahertz). The current cellular systems (including 4G LTE) operate below 6 GHz and since a number of years, is very crowded.

Looking at higher frequency bands is the only way out and a large amount of spectrum is available in the millimeter wave frequency band (24-300GHz) [5] being one the most important prerequisite to launch 5G, since it supports very large bandwidths (in the range of several GHz).

However, this frequency band has its drawbacks. One of them is the well-known Friis transmission formula, where the path loss is higher for higher frequencies, which for millimeter

waves, diminishes the coverage area by a transmitting antenna; another one is the propagation of the waves resembling more a quasi-optical connection between the terminals: the rich scattering is really difficult to realize and the Line of Sight (LoS) component becomes dominant (if not the only present) [38]. Nevertheless, the large amount of spectrum provided by this frequency bands remains very desirable due to its advantages. Therefore, 3GPP designed 5G-NR to be flexible over the full frequency range. Each spectrum band represents unique properties, which means a service provider has a variety of opportunities to balance output, coverage, quality and latency, as well as reliability and spectral efficiency. By joining this bands, 3GPP objective is to support reliable coverage for low frequencies (i.e., below 6 GHz) and high frequencies when high throughput and low latency operations are required (i.e., mmWave coverage).

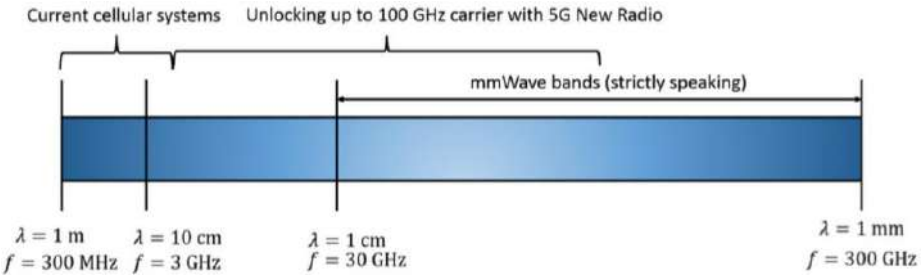


Figure 2.10: Spectrum for current cellular systems and 5G [5].

According to [18][39], in order to provide wide coverage to serve all use cases, 5G requires spectrum across three main frequency ranges, also illustrated in figure 2.10:

- **Sub-1GHz (Low-frequency bands)**: needed to extend high speed 5G mobile broadband coverage across urban, suburban and rural areas and to help support IoT services. The band with highest interest is the 700 MHz band, corresponding to the 3GPP NR band n28. As the bands are not very wide, only a maximum of 20 MHz of channel bandwidth is achieved.

- **1GHz-6GHz (Medium-frequency bands)**: provides a good coverage balance and 5G network capacity via a wider channel bandwidth (up to 100 MHz). The highest interest globally is in the range 3300-4200 MHz, with some regional variations, which 3GPP has designated NR bands n77 and n78. Up to 200 MHz of channel bandwidth per operator can be allocated in a longer term, so that carrier aggregation can be used for the maximum bandwidth.

- **Above 24GHz (High-frequency bands)**: needed for ultra-high speed mobile broadband, without these bands will be impossible to meet the high data rates required. The highest interest is in the range 24.25-29.5 GHz, with 3GPP NR bands n257 and n258 attributed. Channel bandwidths up to 400 MHz are defined for these bands, with even higher bandwidths possible through carrier aggregation. The very fast attenuation of the radio signal due to atmospheric attenuation, especially in adverse weather and poor foliage penetration has brought doubt on the potential to use this range to provide wide area coverage, particularly in the uplink direction where MIMO and beamforming may be not as effective as in the downlink, but field tests and simulations show that mmWave has a crucial role to play in 5G [27].

2.1.2.B Transmission Scheme and Radio Frame Structure

In the release 15, 3GPP defined the operating bands, corresponding to different frequency ranges for downlink and uplink. According to [39], the initial deployments of NR will be based on FR1 range, which is presented in the table below:

The key focus is on new mobile bands including spectrum in the 3.5 GHz range or band n78 (i.e., 3.3-3.8 GHz) that has been assigned in numerous countries [32].

NR operating band	UL : BS receiver - UE transmitter (MHz)	DL : BS transmitter - UE receiver (MHz)	Duplex Mode
n1	1920 - 1980	2110 - 2170	FDD
n3	1710 - 1785	1805 - 1880	FDD
n7	2500 - 2570	2620 - 2690	FDD
n8	880 - 915	925 - 960	FDD
n20	832 - 862	791 - 821	FDD
n28	703 - 748	758 - 803	FDD
n38	2570 - 2620	2570 - 2620	TDD
n77	3300 - 4200	3300 - 4200	TDD
n78	3300 - 3800	3300 - 3800	TDD

Table 2.2: Operating bands defined by 3GPP for 5G-NR in FR1 (Frequency Range 1).

In order to support a wide range of deployment scenarios from large cells with a frequency of sub-1 GHz, up to millimeter wave deployments of very large spectrum allocations, the NR supports flexibility in the OFDM numerology with a subcarrier spacing varying from 15 kHz to 240 kHz with a proportional variation in the duration of the CP. The word ’numerology’

here means the values selected for OFDM design parameters such as Subcarrier Spacing (SCS), Frame/Subframe duration, Transmission Time Interval (TTI) length, CP length, and others.

Instead of a single set of defined values, the NR approach is to allow for dynamic/adaptable numerology. The network should be able to adjust the numerology applied based on traffic pattern, coverage, carrier frequency and other application parameters.

In particular, 3GPP agreed that subcarrier spacing could be chosen according to [40]:

$$\Delta f = 2^{\mu} \times 15_{[kHz]}, \tag{2.1}$$

where Δf is the SCS and μ is the numerology configuration number (integer-value). The following table 2.3 provides detailed information about the NR OFDM transmission numerologies, as agreed in the 3GPP:

The 15 kHz numerology is identical to the one used in LTE, with a slight difference in the number of OFDM symbols per slot, as in LTE is 7 OFDM symbols whilst in NR is 14 OFDM symbols. The duration of radio frame and subframe are established as 10 ms and 1 ms, respectively. A Physical Resource Blocks (PRB) consists of 12 consecutive subcarriers in the frequency domain. A NR radio carrier is limited to 3300 active subcarriers (275 PRB) which results in carrier bandwidths of 50, 100 and 200 MHz for SCS of 15, 30/60 and 120 kHz, respectively [41].

In an OFDM system, to prevent inter-symbol interference, the cyclic prefix is selected larger than the channel delay spread [5]. Generally, the delay spread decreases with the cell size and the cyclic prefix duration needed so that wider subcarrier spacings (that have a shorter cyclic prefix) are more suitable for deployments with smaller cell size. This is closely associated with the fact that smaller cell sizes are designed for higher carrier frequencies as a consequence of severe propagation characteristics and wider subcarrier spacing that make the system resilient to phase noise [5]. Numerologies with wider subcarrier spacings are also optimal for low latency services since the duration of the transmission slot (as set out in table 2.3) is inversely proportional to the subcarrier spacing.

Note: one Physical Resource Block (PRB) is 12 subcarriers for all numerologies.

Frequency range	μ	SCS Δf [kHz]	Frequency Band [GHz]	MIN Bandwidth [MHz]	MAX Bandwidth [MHz]	MIN PRB	MAX PRB	OFDM Symbol Duration with CP [μs]	Slot Duration [μs]
FR1	0	15	0.45-6	5	50	25	270	71.35	1000
FR1	1	30	0.45-6	5	100	11	273	35.68	500
FR1	2	60	0.45-6 24-52.6	10	100	11	264	17.84	250
FR2	3	120	24-52.6	50	200	32	264	8.91	125

Table 2.3: Scalable OFDM numerology for 5G-NR.

The figure 2.11 graphically summarizes the relationships between cell size, carrier frequency, and achievable latency for NR.

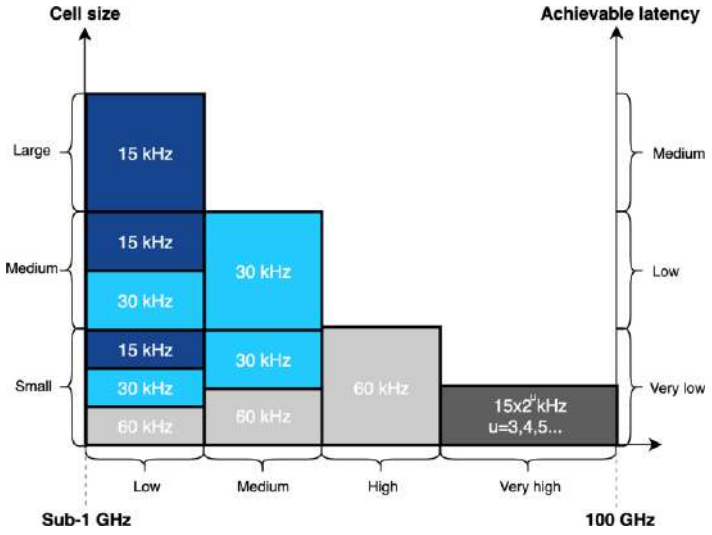


Figure 2.11: The NR numerology for wide range of frequencies and deployment types (adapted from [40]).

Figure 2.12 illustrates OFDM symbols and slots for the different numerologies, where dark symbols depict OFDM symbols with longer CPs (every 0.5ms). It can be seen that narrower SCS numerologies can fit into a slot of a wider SCS numerology. As an example, a 30 kHz SCS has a slot duration of 0.5ms, which can be mapped to two slots (each of 0.25ms) for a 60 kHz SCS. Such nested slot structure and nested PRB-structure facilitates multiplexing of different numerologies in a same cell or for a same UE [36]. This is an important feature for Time Division Duplex (TDD) networks, as the uplink and downlink transmission intervals are lined up in time [5].

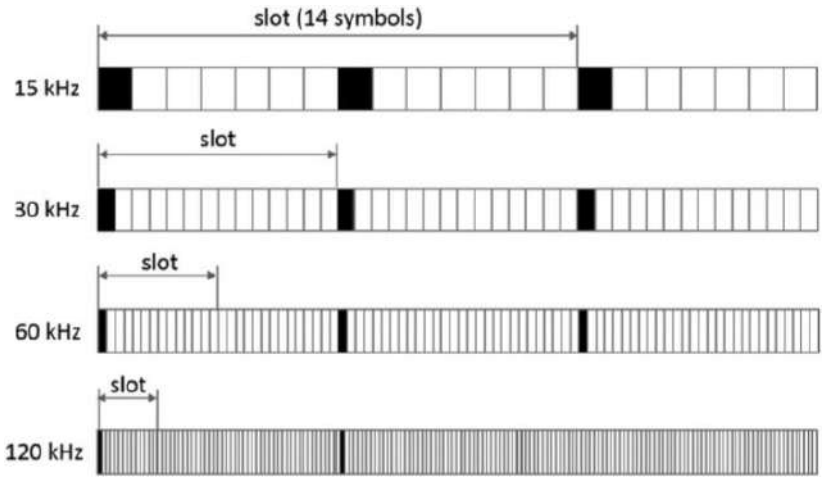


Figure 2.12: 3GPP NR frame structure [40].

2.1.2.C Duplex Scheme

The table 2.2 presents the duplex mode in last column for each of the operating frequency bands. All 5G bands above 3 GHz including the crucial 3.5 GHz and mmWave frequencies will adopt TDD [39], making 5G the first major cellular network implementation of the TDD, whilst Frequency Division Duplex (FDD) has been the dominating duplex scheme since the beginning of the mobile communication era [11].

In FDD operation, downlink and uplink transmissions occur at the same time but using different carrier frequencies, therefore being frequency-multiplexed. In the other hand, TDD has a major advantage in the use of a single frequency band where downlink and uplink occur in alternating time slots, thus being time-multiplexed. A guard time is provided without transmission to permit the switching between transmissions (DL/UL) and, therefore, avoid interference. NR also makes use of dynamic TDD, where a slot can be dynamically allocated by the scheduler to either downlink or uplink transmission.

At lower frequencies, the spectrum allocations are mostly paired, implying FDD transmission. At higher frequencies the spectrum allocations are often unpaired, implying TDD [5]. Due to the flexibility required in the duplex arrangement, NR supports both FDD and TDD operation.

2.1.3 Multi-antenna Transmission

Active Antenna Systems (AAS), also known as Advanced Antenna Systems, have become a viable feature for large scale deployments in mobile networks, as the demand for throughput, improved user experience and ubiquitous coverage from end-users and companies continue to grow [42]. Beamforming and MIMO techniques are powerful tools for improving end-user

experience, capacity and coverage, in a cost-effective way.

Active antenna systems have various advantages. The most flagrant is the reduction of the physical tower space, as a lot of hardware components were eliminated and multiple radio transceivers were integrated inside the antenna, with integrated signal amplifiers built right into the unit. In addition, the ability to electronically tilt transmission beams, controlling independently the phase and amplitude to shape and steer the radiated beam [43]. It is also beneficial for multi-RAT systems where diverse technologies (e.g., UMTS, LTE) coexist in the same frequency band.

Depending on the number of users, mainly two types of multi-antenna systems can be deemed: Single User MIMO (SU-MIMO) and Multi-User MIMO (MU-MIMO). As their name implies, in single- user MIMO the information is transmitted simultaneously between different multiple data layers towards a target UE where each layer is separately beamformed thereby improving peak user throughput and system capacity [42], whereas in multi-user MIMO the difference is mostly the plural number of users, as the base station communicates with multiple devices using a separate stream for each. While SU-MIMO increases the data rate of just one user, MU-MIMO allows to increase the overall capacity as well as having better spectral efficiency (bit/s/Hz) than SU-MIMO [44].

2.1.3.A Beamforming

Beamforming, as mentioned in section 2.1, is an enabling technique that directs the radiation pat- tern of an antenna towards a specific receiving device. Through adjusting the phase and amplitude of the transmitted signals, the overlapping waves will produce constructive (and destructive) addition of the corresponding signals, which can increase the received signal strength and therefore the end-user throughput [45]. When receiving the signal, the UE must also have the ability to collect that specific signal, as the beams are constantly being adapted in phase and amplitude accordingly to the surroundings due to multi-path fading.

There are two basic types of beamforming: digital beamforming and analog beamforming. Analog beamforming uses phase-shifters in the RF domain to send the same signal but with different phases, and the power dissipation is usually lower than in digital beamforming [46]. Alternatively, in digital beam- forming, the transmitted signal is pre-coded in both amplitude and phase during baseband processing before RF transmission, which provides greater flexibility with more degrees of freedom to implement efficient beamforming algorithms and thereby enhancing cell capacity as data can be transmitted con- currently for multiple users using the same physical resource blocks [29]. Digital beamforming has higher power dissipation

and due to the requirement of a separate RF chain for each antenna element it results in a complex architecture and high power consumption [47].

The beam pattern of a mobile communication base station has a major impact on the performance of a cellular network. In classic beamforming, the transmitted or received radio energy concentrated in a specific direction, allied with MIMO schemes that exploits the spatial diversity of the radio channel, are limited to operate generally on the horizontal antenna pattern, whilst the vertical pattern is fixed [48]. However, recent availability of new flexible antenna techniques, such as vertical antenna pattern adaptation, allied with horizontal antenna pattern adaptation, enables a fully dynamic adaptation and control of the antenna pattern in 3 dimensions, which can be specified per PRB and UE, hence offering a better spectral efficiency and making the so-called 3D beamforming highly viable. This feature associated with MIMO capability of employing additional spatial diversity can impact positively the quality of the signal and the number of users served.

Regarding the uplink, the process is a bit different and an important beamforming concept defined by 3GPP comes by, named beam correspondence. In short, it is about the UEs ability to transmit in uplink based in the best direction recommended by the gNB. The UE measures the best DL beam, transmit N candidate UL beams while the gNB selects the best UL beam from the UE transmission and feedback which is the most beneficial so the UE can continue with the beam indicated by the gNB, establishing a beam pair link.

In respect to broadcast, common control channels and cell reference symbols are transmitted via sector beam, a beam with a radiation pattern wide enough (e.g., 90^{o} beam width) to provide coverage in the cell for the radio channels that cannot or must not be beamformed, both vertical and horizontal planes.

All parameters related to the configuration of beams used in a cell are collected in a beam set. The core of such a beam set is the distribution of the SSB beams in the angular space which covers the cell, but without giving the actual values of the beam directions and beam widths. This distribution is called basic beam set, which is illustrated as an example in figure 2.13 and is described as follows:

- basic beam sets consist of rows and columns.
- the number of columns may be different in different rows.
- the total number of transmitted beams has to be less than or equal to the maximum number of SS/PBCH blocks.

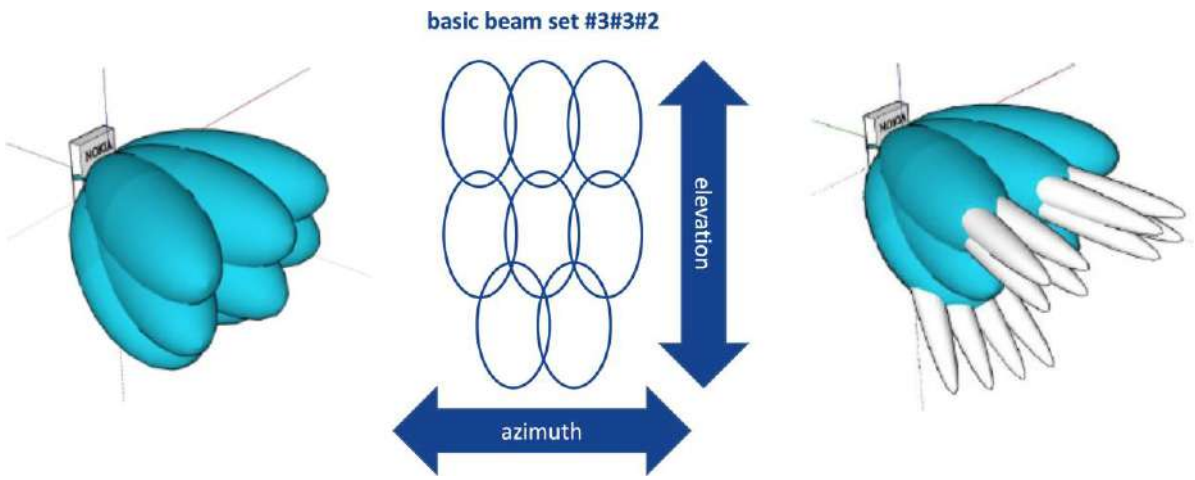


Figure 2.13: Basic beam set #3#3#2.

Each SSB beam has four refined beams implemented, which are used to achieve higher Carrier-to-interference-plus-noise Ratio (CINR) for a single UE, as well as to better separate multiple UEs in MU-MIMO operation. These refined beams carry channel state information, PDSCH, PDCCH, PUSCH, PUCCH, which are illustrated in the figure above.

2.1.3.B Massive MIMO

Massive MIMO promises significant gains in spectral effectiveness for cellular systems, as it was shown by [49] where spectral efficiency grew just about linearly with the number of antennas of MaMIMO. The spectral efficiency grow just about linearly with the number of antennas of MaMIMO [49] and it is related with the SINR improvement due to narrower beams. The high degree of energy concentration in space from the narrower beams increases the signal strength provided to the UE location and less power is spread in other direction, causing lower level of interference; 3D beamforming (beam position can be controlled in three dimensions, enabling individual control of down tilt, hence the improvement of received signal strength and substantial reduction of inter-cell-interference), and multi-user gain (when UEs are placed in different locations, they can reuse the same PRBs, so each UE can be allocated with all available PRB, hence the number of available PRB is multiplied by the number of UEs thus providing multi-user gain).

As already stated in section 2.1, *Massive* simply refers to the large number of antennas in the base station antenna array (typically tens or even hundreds) and MIMO (Multiple-Input Multiple-Output) technology, as the name suggests, is a wireless technology that uses multiple transmitters and receivers to transfer more data at the same time, with which spatial multiplexing is achieved. The extensive number of antenna array provides degrees of freedom

that can be explored alongside with the energy efficiency as the energy is focused in smaller areas [50].

Given the operating frequency, in most 5G cases, in high frequency bands, it is possible to fit a considerable amount of antenna elements in the array, as the inter-spacing between antenna elements should be in the order of the wavelength, at least half of the wavelength ($\lambda/2$) in an equispaced array, to reduce the effect of mutual coupling (an electromagnetic interaction between the antenna elements in an array that causes changes in the radiation pattern and individual input impedance, plus it is inversely proportional to the inter-spacing of antenna elements); and the correlation coefficient between the antenna ports that can be caused by mutual coupling and therefore affect the capacity performance of the MIMO system [51]. Furthermore, inter-element spacing equal or greater or slightly greater to $\lambda/2$ is favored to achieve higher directivity in large antenna array [52], as it results in a larger antenna aperture, therefore, a higher gain is focused towards certain directions and smaller in the vicinity of the main lobe, that becomes narrower, as needed in massive MIMO application. However, this inter-element spacing should not be much greater than half of the wavelength to not led to the presence of grating lobes (unintended radiation beams similar to the main lobe in undesired directions) [38], so there is evidently a compromise between these two opposing factors, where the ideal value will vary among the industry.

As revealed by the relation between antenna elements and wavelength, the antenna element spacing is considered a function of frequency, therefore, these antenna panels can have a very reduced size at high frequencies.

Polarization diversity also plays an important role, being a coveted system objective, providing the ability to different kinds of antenna polarizations such as horizontal, vertical or both left-hand and right-hand circular polarization. To achieve this diversity, the antenna radiating element consists of two ports that radiate orthogonal polarizations, obtained by controlling the relative phase and amplitude of each port [53]. The ideal configuration of this cross-polarized antennas is achieved by slanting one of the elements 45 degrees to the left and the other 45 degrees to the right, improving equality in received signal levels, throughput and coverage in urban environments [54]. Another advantage of this dual-polarization is the reduction of transmit-array size by half compared to a spatially separate single-polarized transmit-array [55].

In MaMIMO, there are some principles regarding the antenna elements and the transmitter, as it is stated in [21]. The capacity increases with the number of antenna ports, that is, increasing the number of independent data streams (layers) allows to send data to multiple UEs in parallel

but, conversely, leads to an increase of the power consumption and costs. Furthermore, the number of antenna elements defines the antenna gain, which controls coverage, that is, more antenna elements results in more coverage.

In order to obtain the benefits of additional antennas and to fully enjoy the capacity gain offered by MaMIMO, it is needed to characterize the spatial channel between the antenna elements and the UE, generally referred as Channel State Information (CSI) [16]. Yet, increasing the number of antennas means also growing of the overhead of acquiring CSI [56]. TDD plays an important role for reducing the overhead of CSI by using the reciprocity of the channel [57]. As the channel is the same in both directions (uplink and downlink) and TDD uses the same frequency band, reciprocity means it can be in only one direction, making the uplink pilot signal the most appropriate choice [16] as it can be sent directly from the UE to all the antenna elements. This spatial transfer functions and information are then collected and gathered in a matrix that is constantly being updated by the feedback of the users.

2.2 Propagation Models

Consumer demands shape the evolution of mobile broadband services, and to fulfil the requirements of the new generation there are a wide variety of network aspects and propagation scenarios that have to be modelled. For this reason, it is important to have model frameworks that reproduce radio channel responses as close to reality as possible [58], including dense urban environments, urban, rural, indoor, and related links topologies between these scenarios. Moreover, it is required a previous knowledge of radio wave propagation characteristics and its effects such as reflections, diffractions and scattering, as their interference with buildings, walls, objects, moving bodies and clutter in general can result in multi-reception of the same signal with delay or driving to signal fading. The use of the millimeter-wave spectrum poses new challenges to the network, as they have limited propagation ranges, increased atmosphere attenuation and high sensitivity to events that can cause service blocks [59]. Actually, several state-of-the-art radio propagation models [58] are yet to be validated and recognized by the scientific community [60] as it is important to use a model that fits and satisfies all the requirements with minimal complexity. Propagation models are essentially split into empirical and deterministic models.

On the one hand, empirical models are formulated based on extensive measurement campaigns and experiments, being statistically adjusted for the data collected at the side under study. This type of models is simple and easy to use, thus achieving predictions of values without recourse to great computational processing effort, as they do not take into account the theory of electromagnetic wave propagation. As this model is based on measurements, it is naturally a least accurate model due to prediction errors that can affect negatively the radio network planning. Examples of this kind of models are *Okumura-Hata, COST 231-Hata* and *Standard Propagation Model (SPM)* represented in figure 2.14.

On the other hand, deterministic models rely on detailed information data about the propagation environment, like object materials, obstacles, positioning, allowing to predict its characteristics at every point in space and thus providing more accurate results than empirical models. This accuracy requires a high computational effort for the complex calculations of the electromagnetic field, and their challenge lies mostly on minimizing the memory and computational burden. The electromagnetic solver accounts relative permittivity and conductivity of buildings and terrain for the electromagnetic properties, as they are frequency dependent [59]. These models are based in theoretical predictions, which are achieved due to Ray Tracing (RT) techniques that consider several propagation phenomena (e.g. direct ray, diffraction, reflection and scattering) determined by geometrical optics, geometric theory of diffraction, and uniform theory of diffraction approximations of magnetic fields [61].

A representative comparison scheme between the Standard Propagation Model and the Ray Tracing Model is represented in the figure 2.14.

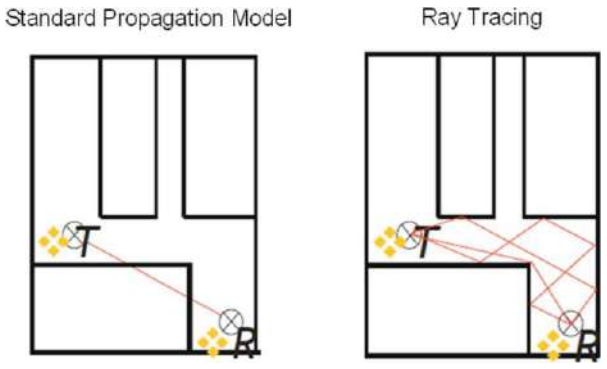


Figure 2.14: Representative schemes of the SPM and Ray Tracing propagation models [62].

2.3 Types of Databases

Although network planning studies are based on path loss calculation and propagation models, the geographic database also plays a major role, since the predictions are performed using information from these terrain databases. These databases have information about the environment, that differ from the type of scenario, that can be urban, rural or even indoor, which each of them has a different kind of accuracy and detail regarding the obstacles.

The most basic type of database is a 2D database, that usually gathers files like the Digital Terrain Model (DTM) and clutter classes file, which will be seen more in detail in the next chapter.

This type of database can be upgraded to 2.5D by combining the 2D model and an additional layer of average heights per clutter class, named clutter heights, where some classes like vegetation will have less average height than high buildings. This database type is produced mostly for urban and suburban areas with multitype buildings, vegetation and other obstacles that have an essential effect on wave propagation [63].

The most powerful, accurate and consequently costliest model is the 3D model, that takes into account all the possible obstacles and objects in the urban environment, being able to distinguish buildings by their shape and subdividing them into small classes within the type of building, with the objective of being as close as possible to reality.

Chapter 03: RF planning tool (Atoll)

In this chapter, a description of the planning tool used is made firstly, followed by the input parameters regarding the site, transmitter and cell, as well as the propagation model. Subsequently, the coverage area of study is analyzed, alongside with the geographic database. The different antennas used are also described, and lastly, the definitions of the predictions carried out in this study.

3.1 Radio Network Planning Tool

For planning a mobile network, the three main objectives are: **mobile network coverage**, **DL/UL quality** and **capacity**. 5G-NR is no different, and these objectives are targeted for better results than the legacy mobile network generations.

The *Atoll* tool is a fine-tuned network planning software from *FORSK* company, this tool includes advanced multi-technology network planning feature and radio access technologies such as 5G NR, LTE, NB-IoT, UMTS, GSM and CDMA; integrated single RAN-multiple RAT network design capabilities for the previous mentioned cellular radio access technologies [64].

Atoll working environment is presented below in figure 3.1.

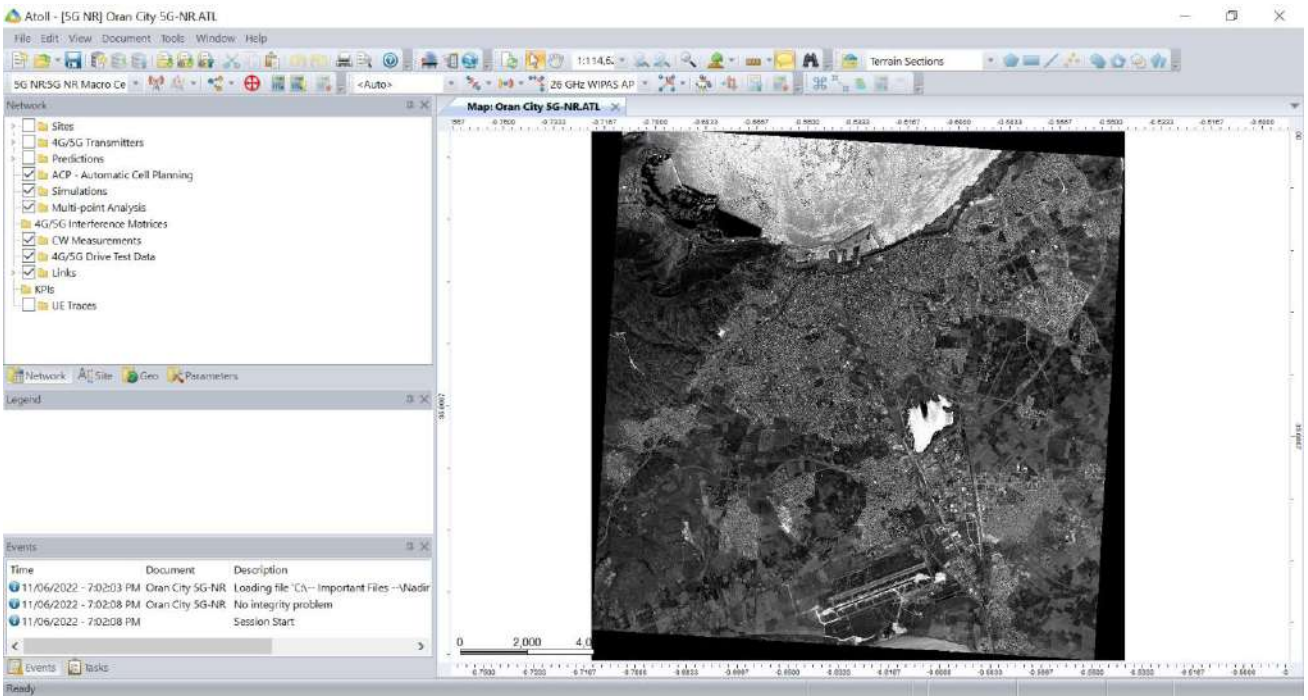


Figure 3.1: *Atoll* working environment (Oran City topographic view).

This study is made by means of coverage predictions, where the signal levels are calculated in every pixel. The coverage of a mobile network is directly related to the range of the received signal in conditions that still allow the reception and decoding of the signal. This signal must be strong enough to resist attenuation in air transmission, taking into account the noise of the receiver and its sensitivity.

Before making predictions, it is necessary to create the network. The information related to the propagation model, sites, cells, and transmitters must be filled in, followed by the clutter and morphology classes information.

3.2 Propagation Model

The initial planning of every radio access network starts with a radio link budget. As the name implies, a link budget is simply the accounting of all of the gains and losses from the transmitter, through the medium to the receiver in a telecommunication system.

Using this knowledge, it is possible to assess the levels of power and gain once the system is installed and operating, and in case of insufficient signal or incorrect operation, to take corrective measures to ensure that the system works satisfactorily, aiming for the cheapest solutions.

A good link budget is essential for a functioning link, and it is divided generally in 3 elements :

- **Transmitting side**: includes transmitting power; antenna gain; transmitter feeder and associated losses (feeder, connectors, etc.).
- **Propagating side**: free space path losses, miscellaneous signal propagation losses (these include fading margin, polarization mismatch, losses associated with medium through which signal is travelling, among other losses...).
- **Receiving side**: antenna gain, receiver feeder and associated losses (feeder, connectors, receiver sensitivity, etc.).

The link budget takes essentially the form of the following equation :

$$P_{Rx} = P_{Tx} + G_{Tx} + G_{Rx} - (L_{Tx} + L_{Rx} + L) \tag{3.1}$$

where:

- P_{Rx}: received power [dBm]
- P_{Tx}: transmitting power [dBm]
- G_{Tx}: power gain of the transmitting antenna [dBi]
- G_{Rx}: power gain of the receiving antenna [dBi]
- L_{Tx}: transmitter feeder and associated losses [dB]
- L_{Rx}: receiver feeder and associated losses [dB]
- L: electromagnetic wave propagation attenuation [dB]

The attenuation loss L is the hardest to assess in a radio link budget due to electromagnetic waves propagation complexity. To take into account the different physical phenomena propagations such as diffraction; dispersion; reflection; penetration over obstacles; and absorption, some propagation models were studied and developed, allowing the average value

of propagation loss to be determined. As stated in section 2.2, the propagation models can be based on measurements and statistical adjustments, called empirical models, or based on physical laws and electromagnetic theory, called deterministic models. At present, these deterministic models are obtained by ray tracing electromagnetic method, which is, unfortunately, characterized by high time consumption due to the high computation effort. While the latter model requires a detailed information about the propagation environment, empirical models are simpler and require less computation effort. Based on expensive measurement campaigns and statistical analysis makes them highly environmentally dependent, as one empirical model cannot be used for different environments, since it will lead to significant prediction errors, thus less accuracy. Despite this, the easy implementation and fast calculation time makes this model very popular since most of them are based on a simple formula.

For this thesis, the Atoll Standard Propagation Model (SPM) was adopted. SPM is an empirical model and it was developed based on the Hata path loss formulas. This model is apt for the 150 - 3500 MHz frequency band, which evidently comprises the 3.5 GHz or n78 band, defined by 3GPP and previously mentioned in sections 2.1.2.A and 2.1.2.B. It determines the large-scale fading of received signal strength over a distance range of one to 20 km. SPM supports GSM, UMTS, CDMA2000, LTE, WiMAX, Wi-Fi and NR. This model counts with automatic calibration, available in the radio planning tool.

The Standard Propagation Model is based on the following path loss formula, where each *K* is influenced by the type of terrain, diffractions, the height of both receiving and transmitting antennas, and the clutter classes:

$$P_R = P_{Tx} - K_1 + K_2 \log(d) + K_3 \log(H_{Tx}eff) + K_4\, DiffractionLoss + K_5 \log(d) \log(H_{Tx}eff) + K_6 H_{Rx}eff + K_7 \log(H_{Rx}eff) + K_{clutter}\, f(clutter) + K_{hill,LOS} \quad (3.2)$$

where:

- P_R: received power [dBm]
- P_{Tx}: transmitted power [dBm]
- K_1: constant offset [dB]
- K_2: multiplying factor for log(d)
- d: distance between the transmitter and the receiver [m]

- K_3: multiplying factor for $\log(H_{Txeff})$
- H_{Txeff} : effective height of the transmitter antenna [m]
- K_4: positive multiplying factor for diffraction calculation ($K_4 \geq 0$)
- *DiffractionLoss: losses due to diffraction over an obstructed path [dB]*
- *K5: multiplying factor for log(d) · log(HT xeff)*
- *K6: multiplying factor for HRxeff*
- *K7: multiplying factor for log(HRxeff)*
- H_{Rxeff} : mobile antenna height [m]
- $K_{clutter}$: multiplying factor for $f(clutter)$
- $f(clutter)$: average of weighted losses due to clutter
- $K_{hill,LOS}$: corrective factor for hilly regions (= 0 in case of NLoS)

All these parameters can be configurable by the user for specific studies yet most of the parameters are already pre-defined and calibrated based on extensive measurement campaigns and experiments in the biggest cities and capitals, which are taken by default by most of the vendors when planning radio networks.

The parameters taken by default in this project are shown in the figure 3.2.

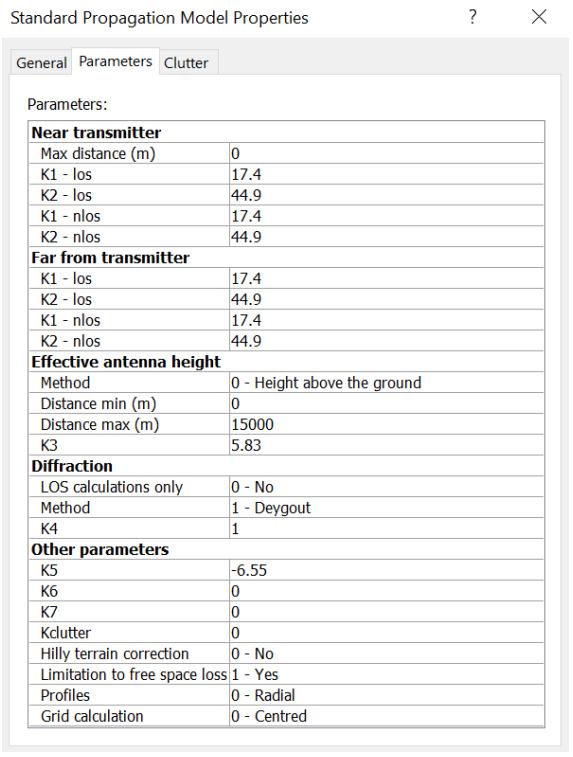


Figure 3.2: Standard Propagation Model parameters.

To a more realistic approach, the losses by clutter class were taken into account and adjusted to the band used. These clutter classes, which will be shown in a later section, also have a specific attenuation for each type of clutter, in this case following Nokia internal guidelines, and are configured together in the SPM model, defined in the following figure:

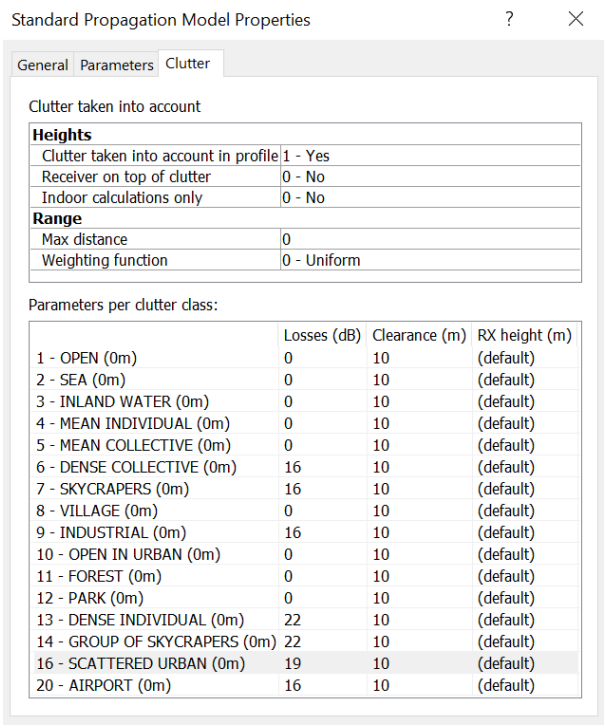


Figure 3.3: Standard Propagation Model clutter parameters.

3.3 Network Configuration Parameters

Atoll enables the design and configuration of the network, including the base station, transmitter equipment and cell parameters.

The design is started by the geographical introduction of the site, followed by the base stations and its parameters.

Afterwards, in the cell section, the remaining parameters for the base stations are configured. Some of these parameters are frequency band, maximum power, coverage threshold values, use of diversity, numerology, traffic loads, among others.

Some parameters maintain the same configured values regardless of location or band. In table 3.1, some general parameters throughout every equipment in the project are presented, followed by a brief parameter overview.

- **Main Resolution**: The resolution determines the size of a pixel, where a smaller pixel provides a higher resolution, which in turn requires more processing. For every prediction, the resolution used is 5 meters, as well as the resolution of every geographic database used. Taking into account that the study area (**Oran City full cluster**) is around 186.1 km^2, this resolution is enough to achieve accurate results.
- **Antenna Height (HBA)**: Represents the height of the antenna above the ground and includes the height of the building which the transmitter is situated (defined cell by cell).
- **Frequency Band**: The frequency band selected is the n78 band, commonly referred to as the 3.5 GHz 5G band, defined by 3GPP [32]. This band is chosen as recommended by GSMA guidelines for MENA region (Algeria included).
- **Carrier**: The carrier of the cell in the frequency band. This carrier has center frequency (NR-ARFCN 621667) of 3.5 GHz, a bandwidth of 50 MHz and operates with TDD duplexing method.
- **Carrier Bandwidth**: The carrier bandwidth is defined as 50 MHz, half of the highest bandwidth available in the simulator.
- **Layer**: 5G NR networks can be deployed in multiple layers of heterogenous cells, i.e., of different sizes (macro, micro, small cells, and so on), which they can be prioritized during cell selection and has a maximum speed assigned to restrict the user connection to the cells of this layer. Although, for this study, only macro layer was available for the serving cells.
- **Radio Equipment**: The 5G NR gNB below 6 GHz is a pre-defined radio equipment available in the simulator, with configured bearer selection thresholds and respective modulations schemes, channel coding rates, bearer efficiency and MIMO gains.
- **Diversity Support**: Either for downlink or uplink (transmitting and receiving), this parameter allows to specify the type of antenna diversity technique, that can be none, SU-MIMO and/or MU-MIMO.
- **Maximum Traffic Load**: For either downlink or uplink, this parameter represents the maximum traffic load not be exceeded, for which the entered value represents the cell traffic load limit.

Parameter	Input
Main Resolution	5 m
Antenna Height	Defined cell by cell (meters)
Frequency Band	n78 (3.5 GHz)
Carrier Bandwidth	50 MHz
Layer	Macro
Radio Equipment	5G NR gNB below 6 GHz Diversity Support (DL/UL)
MIMO Type	SU-MIMO / MU-MIMO
Maximum Traffic Load (DL/UL)	100%

Table 3.1: General parameters configured in *Atoll*.

3.3.1 Site Parameters

The site is simply the geographical location of the base station, where the antenna and all the electronic communications material are located typically on a radio mast, tower, or other raised structure. For simulations where active antenna systems (AAS) are used, the RF modules are located on the tower next to the antennas and therefore are not considered losses regarding the feeder cables.

Sites were introduced in directly in the software and imported from *Excel* format tables. The list of sites was chosen based on the most important areas in Oran (Airport, city center, port …etc.), the full list of existing sites (based on 4G operating sites) is more than this but we were limited this list in order to facilitate the calculations ang get fast results on the most important areas of Oran city.

Name	Longitude	Latitude	Support Height (m)
Place 1er Novembre	-0.64986	35.7038	28
Larbi ben Mehidi	-0.64105	35.70192	25
Port	-0.64236	35.70881	54
: : :	: : :	: : :	: : :
Airport	-0.60667	35.62042	20

Table 3.2: Site parameters configured in *Atoll*.

The deployment area where the site is located will be detailed further ahead.

3.3.2 Transmitter Parameters

Once the site is configured, the transmitters can be inserted. Some of the transmitter parameters (related to AAS selected) will be modified from prediction to prediction, but will be properly identified. Hence, the description of most of the parameters will be summarized here, as well as their values.

Parameter	Input
Antenna Height	Defined cell by cell (meters)
Azimuth (deg)	Defined cell by cell (degree)
Mechanical Down tilt	0 (degree)
Number of Transmission Antennas	16 / 32 / 64
Number of Reception Antennas	16 / 32 / 64
Number of Power Amplifiers	16 / 32 / 64
Noise Figure	3 dB
Main Propagation Model	SPM - Macro layer

Table 3.3: Transmitter parameters configured in *Atoll*.

- **Azimuth**: The azimuth refers to the rotation of the whole antenna around the north (the vertical axis), it is defined cell by cell, chosen sites has between 2 to 3 sectors (cells).
- **Mechanical Down tilt**: The term mechanical down tilt refers to the physical inclination of the antenna's angle along a single horizontal plane. This parameter is fixed at zero degrees (0^{o}) for all sites since the active/advanced antennas have the ability to electronically tilt transmission beams, thus providing more flexibility and greater freedom to maximize the quality of the service.
- **Number of Transmission Antennas**: This parameter represents the number of transmission antenna ports, or Transceiver (Tx), used for transmission in MIMO predictions and will vary accordingly to the station template used. 16, 32 and 64 antenna ports are available for study.
- **Number of Reception Antennas**: This parameter represents the number of receiver antenna ports, or simply Receiver (Rx), used for reception in MIMO predictions and will vary accordingly to the station template used. 16, 32 and 64 antenna ports are available for study.
- **Number of Power Amplifiers**: The number of power amplifiers corresponds to the number of independent sources of power to which the physical antenna ports are connected, in MaMIMO and 3D beamforming antennas. Usually, each antenna port is fed

by a dedicated power amplifier, which means that the number of ports is usually the same as the number of power amplifiers in the antenna. In this case, 16, 32 and 64 power amplifiers are available.

- **Noise Figure**: This parameter is directly related with the transmitter equipment and describes the total amount of noise that the transmitter contributes to the RF signal being received. The noise figure is defined at 3 db.
- **Main Propagation Model**: This parameter is selected accordingly to the propagation model defined in section 3.2, SPM with 2D database.
- **Beamforming Model**: This parameter will depend on the 5G station templates used, duly indicated with the respective model, beam width and beam set configuration.

3.3.3 Cell Parameters

While the transmitter parameters allow to configure the equipment used for transmission and data reception, the cell parameters allow to define the RF channel, with all its characteristics, on a transmitter. Thereby, most of the parameters that were defined will be presented in the table below, with a brief explanation.

Parameter	Input
Cell's Maximum Power	52 dBm
Minimum SS-RSRP	-121 dBm
Traffic Numerology	1 (30 kHz)
Scheduler	Proportional fair
Number of Users (DL/UL)	1 (SU-MIMO) / 10 (MU-MIMO)
Traffic Load (DL/UL)	1
Beam Usage (DL/UL)	Automatic

Table 3.4: Cell parameters configured in *Atoll*.

- **Cell's Maximum Power**: The predefined value, 52 dBm, is associated with the 5G MaMIMO module antennas equipment selected for the study case.
- **Minimum SS-RSRP**: The minimum SS-RSRP required for a user to be connected to the cell. This value is granted as a threshold when a coverage prediction is made, determining whether or not a user is within the cell's coverage or not. This value is pre-defined in telecom vendors internal guides.

- **Traffic Numerology**: The numerology used by the cell for traffic channels (PDCCH, PDSCH and PUSCH).
- **Scheduler**: This parameter represents the scheduler used by the cell for bearer selection and resource allocation. Proportional fair scheduling method allocates the same number of resources to all the users with a maximum throughput demand.
- **Number of Users**: Represents the number of users connected to the cell in downlink and uplink. This parameter value will depend on the prediction made (SU-MIMO or MU-MIMO).
- **Traffic Load**: For either downlink or uplink, this parameter represents the traffic load of the cell. It is selected with the maximum value in order to assess the predictions in full load capacity.
- **Beam Usage**: For either downlink or uplink, this parameter represents the repartition of each beam index in percentage. For downlink it is the percentage of the traffic load carried by each traffic beam, while for uplink it represents the percentage of the uplink noise rise received by each traffic beam. This parameter is shown as *Automatic* since the beam usage ratios can be automatically calculated based on the surface areas covered by the various beams within a cell with respect to the total best server surface area of the cell.

3.4 Deployment Area and Inputs

Mobile communications networks are designed to provide coverage in urban and rural areas so that users can access to voice, data, and video services.

For this coverage, mobile communications networks are based on the idea of cells, i.e., the geographical area that is covered by a base station in a cellular network.

In this thesis, the total area of approximately 186.1 km^2 representing the large city of Oran, west Algeria is taken for the study and it can be seen in the figure below. This area was chosen for the purpose of studying the impact of beamforming and massive MIMO antennas in an urban and suburban environment.

Network planning studies are based on path loss calculation first of all and require an accurate prediction of the propagation phenomena. Although this accuracy relies on the propagation model, the quality of the geographic database is equally relevant. In *Atoll*, the terrain database like Digital Terrain Model (DTM), as well as the ambient database like clutter classes and clutter heights are the inputs of geographic data used in the predictions as described below.

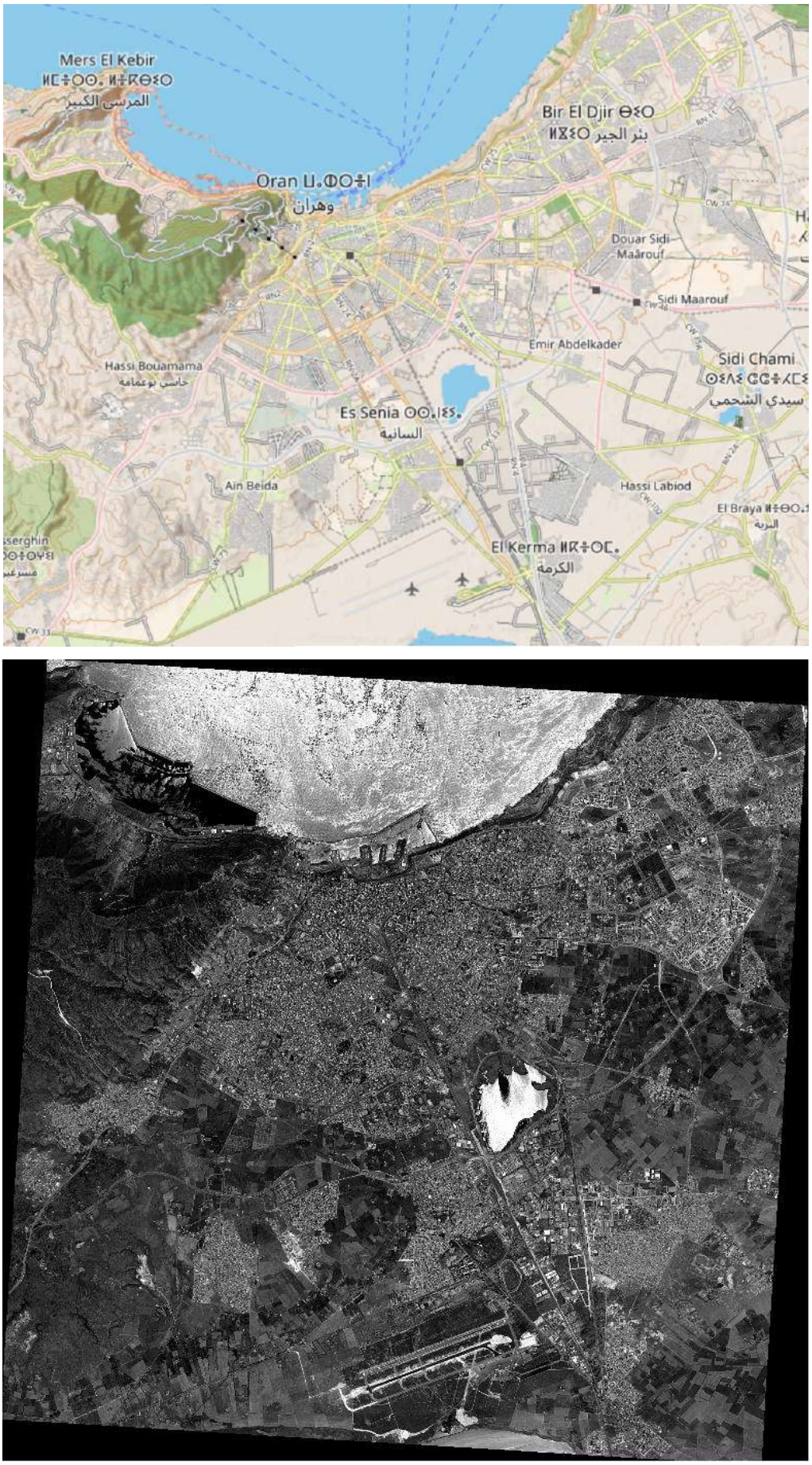


Figure 3.4: Deployment area (Greater Oran City), standard and satellite image maps

3.4.1 Digital Terrain Model

The Digital Terrain Model (DTM), also known as Digital Elevation Model (DEM), is a topographic model that contains the elevation data of the terrain. As it refers to the ground altitude above sea level, vegetation, buildings and other object materials are removed digitally leaving just the underlying terrain. DTM is useful to determine the reception and transmission site altitude, and it is automatically taken into account by the propagation model during computations.

This file gives a terrain elevation value for each image pixel, depending on the resolution, on this case 5 meters, and it is illustrated in the figure below.

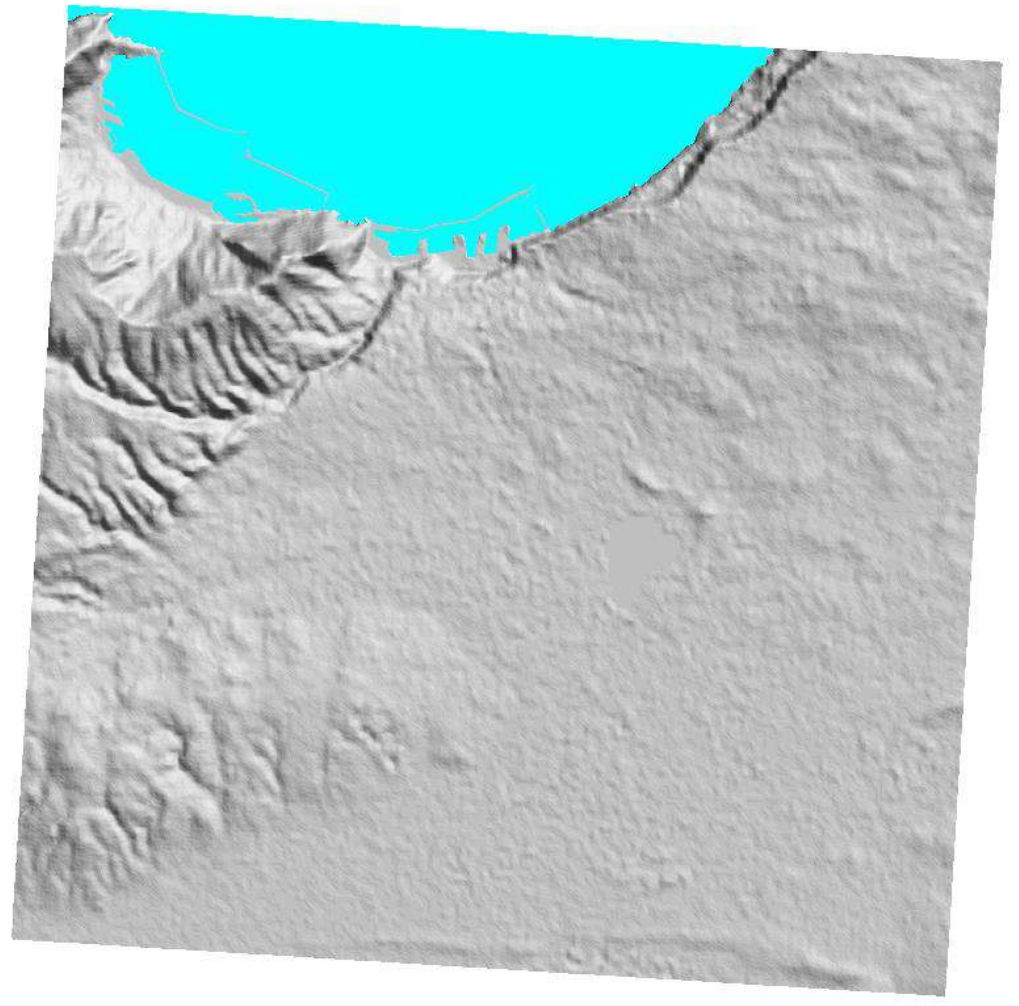


Figure 3.5: Digital Terrain Model (DTM).

3.4.2 Clutter Classes

The geographical distribution of the various environments is given by the clutter classes. Figure 3.6 shows the different number of environments characterized in the clutter classes file, that are taken into account by the propagation model during computations.

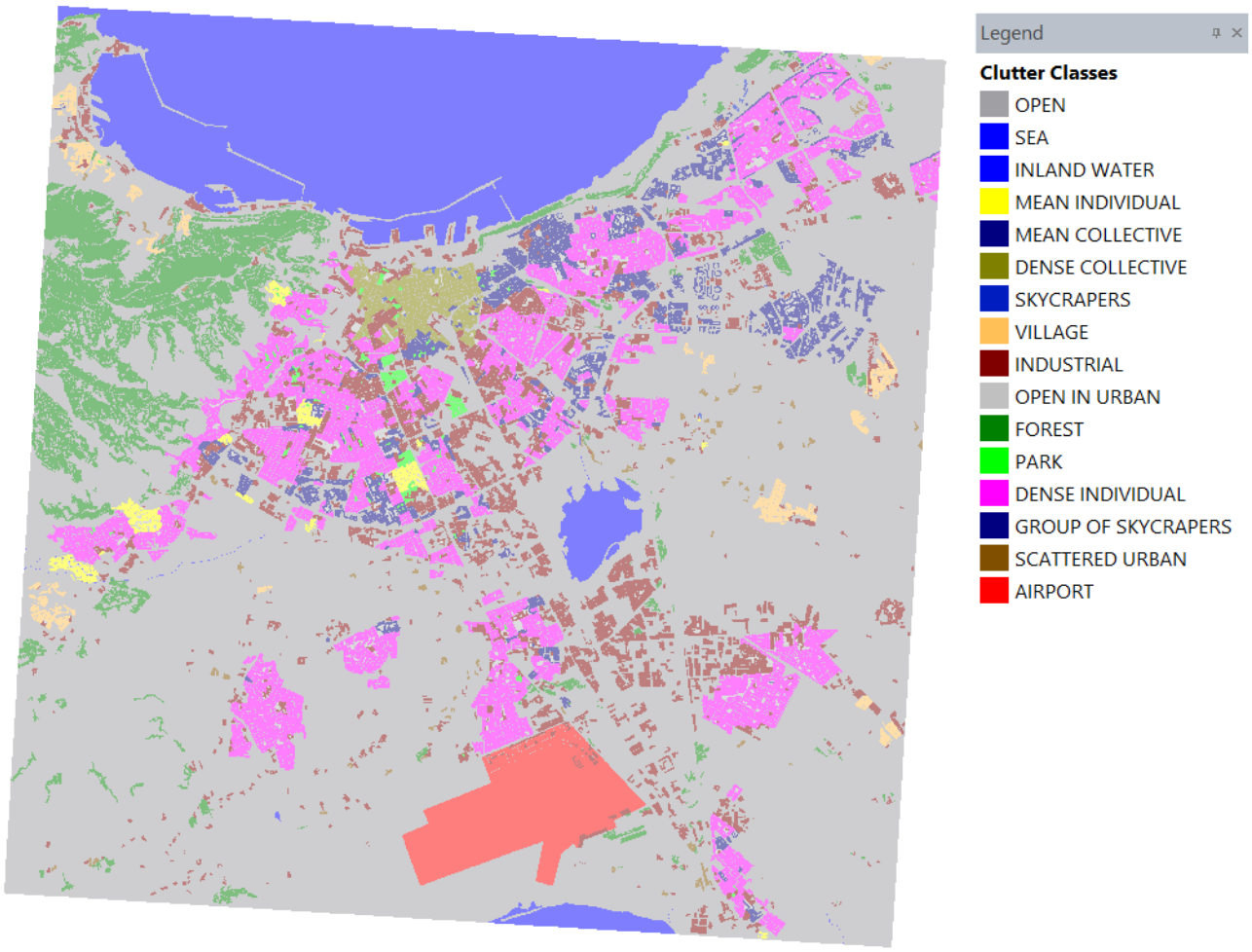


Figure 3.6: Clutter classes.

Atoll uses the clutter classes file to determine the clutter class. Each pixel in a clutter class file contains a code (up to 255 codes) that in turn corresponds to a clutter class [70].

For each of this clutter classes, an attenuation value is assigned, previously shown in figure 3.3. With this input files, the predictions can achieve values closer to the real values of the field.

Table 3.5 represents the correspondences between codes and clutter classes names and the different area percentage of each clutter class. Based on this information, it can be concluded that the area of study is mainly dense urban according to building structures, and the rest considered as open spaces, where the vegetation (despite being named forest) is of low density and extension, so its attenuation is not significant when it comes to path loss calculations, that's why its clutter loss is deemed as null.

Name	Surface (km²)	Percentage (%)
OPEN	133.03418	59
SEA	28.50195	12.6
INLAND WATER	2.40057	1.1
MEAN INDIVIDUAL	0.87592	0.4
MEAN COLLECTIVE	5.36325	2.4
DENSE COLLECTIVE	1.68037	0.7
SKYCRAPERS	0.0852	0
VILLAGE	1.50432	0.7
INDUSTRIAL	12.33002	5.5
OPEN IN URBAN	1.61692	0.7
FOREST	11.73672	5.2
PARK	0.5685	0.3
DENSE INDIVIDUAL	18.93352	8.4
GROUP OF SKYCRAPERS	0.53902	0.2
SCATTERED URBAN	0.54507	0.2
AIRPORT	5.6284	2.5

Table 3.5: Clutter classes.

3.4.3 Clutter Heights

Clutter height maps describe the altitude of the clutter over the Digital Terrain Model (DTM) with one altitude defined per pixel. This file map enhances the precision of the prediction, as each clutter classes can have different heights within a single clutter class. The resolution of this map is also five meters. Actually, for this particular map of Oran greater city area we don't have the clutter heights but a complete vectors map (streets, roads and boundaries) as given on Figure 3.7.



Figure 3.7: Vectors (streets, roads and boundaries)

3.5 Antennas

As the demand for throughputs, enhanced user experience and extensive coverage continues to grow, the operators are developing and meeting these requirements by upgrading the capacity and coverage of their radio networks. One of the technologies developed is the active antenna systems (AAS), or advanced antenna systems, thereby enabling beamforming and MIMO techniques, previously proven methods for end user experience improvement and enhancement of capacity and coverage. In this study, we used active antenna systems (featuring MIMO and beamforming). The purpose is to study the impact regarding the main technologies explored in 5G NR.

The 3D beamforming model enables beamforming in both horizontal and vertical planes. This model is based on predefined beam radiation patterns in which each beam pattern usually has a different azimuth and tilt. In most telecom vendors radio units operating below 6 GHz, it is implemented digital beamforming.

In *Atoll*, 3D beamforming represents uniform planar array antennas with antenna elements aligned horizontally and vertically across a two-dimensional plane. Each 3D beamforming antenna is defined by its operating frequency range, the number of antenna elements (also known as physical antenna elements), the number of antenna ports (also known as logical antenna elements, always less than the number of physical antenna elements), polarization, antenna element spacing and the radiation patterns of all the beams that the antenna can form.

A distinction is made between the antenna model and the beam pattern: 3D beamforming models represent the physical beamforming antenna equipment, which produces multiple antenna patterns; 3D beamforming patterns represent the beam patterns that are produced by the beamforming model. The beams are calculated and generated by the beam generator available in *Atoll*.

In table 3.6 is presented some of the parameters that distinguish the 3D beamforming antennas used.

Parameter	AAS16	AAS32	AAS64
Rows (M)	12	12	12
Columns (N)	8	8	8
Polarization	Cross-polar		
Number of Antenna Elements	16	32	64
Number of Transmission Antenna Ports (Tx)	16	32	64
Number of Reception Antenna Ports (Rx)	16	32	64
Data streams (up to)	8	16	16
Basic Beam Set	#8	#8	#8

Table 3.6: Active antennas parameters (Rows (M) and Columns (N) represent the number of rows and columns of antenna elements within the panel, respectively)

Every 3D beamforming antenna generates 50 beams, 25 control channel beams and 25 traffic channel beams, each of them assigned with an azimuth, electrical down tilt, and the number of horizontal and vertical antenna elements used to form the beam pattern. These 40 beams include the control channel beams (used for the SS/PBCH block) and the traffic channel beams (used for PDCCH and PDSCH). An example of one of the beams can be visualized featuring its horizontal and vertical pattern in the figure

3.9. The antenna gain will vary according to the chosen beam set, between 19.7 and 23.6 dBi.

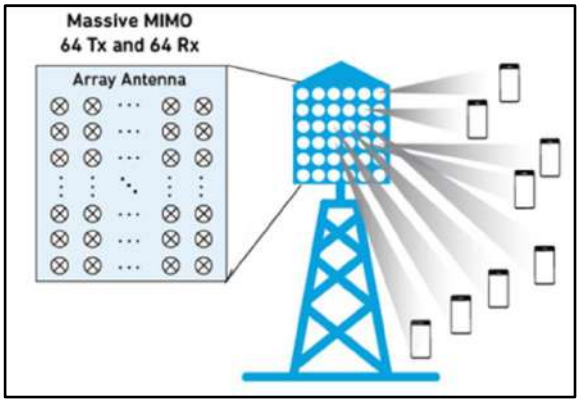


Figure 3.8: Massive MIMO antenna for 3.5GHz band with 64Tx [21].

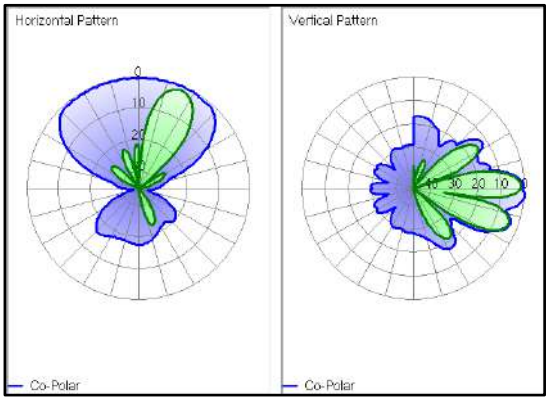


Figure 3.9: Horizontal and vertical pattern of one of the beams.

3.6 Traffic Parameters

Every coverage prediction has associated several parameters regarding the traffic, namely the user's profile, the type of service, the user's mobility and the terminal used by the user.

A wide range of services are available in *Atoll* but for this study, broadband matters the most, since this service is the greatest target in 5G NR deployment.

The broadband service has its characteristics as presented in the table below:

Parameter	Input	
	Downlink	Uplink
Highest modulation	256 QAM	64 QAM
Lowest modulation	QPSK	QPSK
Highest coding rate	0.99	0.99
Lowest coding rate	0.1	0.1

Table 3.7: Broadband service parameters.

The user's terminal is a mobile phone that operates below 6 GHz, previously configured with parameters as shown below:

Parameter	Input
Min Power	-40 dBm
Max Power	23 dBm
Noise Figure	8 dB
Number of Transmission Antennas (Tx)	1
Number of Reception Antennas (Rx)	1

Table 3.8: Terminal parameters.

The user's profile is classified as pedestrian type, equipped with the terminal UE below 6 GHz mentioned above, where the main service is broadband. The receiver's (user) height is set to 1.5 meters, an average height for users in the street.

3.7 Predictions

5G NR coverage predictions available in *Atoll* are used to assess the effective signal levels, signal quality, and throughputs. In this operation, each pixel is considered a non-interfering user with a defined service, mobility type, and terminal, which will be detailed in the following sub section.

These coverage predictions are calculated using download traffic loads and the uplink noise rise values defined at the cell level, previously set, as well as traffic parameters suchlike user profile, mobility, service and terminal properties.

In order to assess the signal levels and signal quality, four types of coverage predictions are available:

- **Network Coverage**: Predicts the effective signal levels of different types of 5G NR signals in the study area. *Atoll* determines the serving cell for each pixel using the standard cell selection mechanism, coloring the pixels if the display threshold condition is fulfilled. This coverage prediction is represented by the **SS-RSRP** prediction.

- **Network Quality**: Predicts the interference levels and signal to interference levels in the study area. The pixel is colored if the display threshold condition is fulfilled. In downlink, the CINR is calculated for different channels using their respective transmission powers and by calculating the interference received by other channels from interfering cells while the in uplink it is calculated using the terminal power and the uplink noise rise values stored in the cell properties. This prediction will be represented by the **PDSCH CINR** levels.

- **Service Areas**: Calculates and displays the 5G NR radio bearers based on CINR for each pixel. The downlink or uplink service areas are limited by the bearer selection threshold of the highest and lowest bearers of the selected service. In turn, each of these radio bearers correspond to a modulation scheme, that will serve as an assessment for this type of coverage prediction.

- **Network Capacity**: Calculates and displays the channel throughputs and cell capacities based on CINR and bearer calculations for each pixel. *Atoll* determines the total of symbols in DL and UL frames from the information previously set in cell parameters. Then, it determines the highest bearer at each pixel and multiplies the bearer efficiency by the number of symbols in the frame to determine the peak Radio Link Control (RLC) layer throughputs. The measurement is made in RLC as every transport block in the cell is delivered to higher layers by the RLC, regardless if they carry user plane or control plane data. The assessment will be made by the effective RLC throughput measure, which is the peak RLC layer throughput reduced by the retransmission due to errors, or the BLER (Block Error Rate, the ratio of the number of erroneous blocks received to the total number of blocks sent).

In *Atoll*, there is 2 different types of gains applied to SU-MIMO and MU-MIMO configurations: diversity gain and capacity gain. The diversity gain is applied to the CINR level and takes into account the number of transmission and reception antennas applied on the signal, improving the CINR, whereas the capacity gain is applied to the throughput and takes not only the number of antennas into account but also the number of MIMO users that share the same resources. In MU-MIMO, schedulers are able to allocate resources over spatially multiplexed parallel frames in the same frequency-time resource allocation plane. The proportional fair scheduler chosen can apply an extra gain, increasing the average cell throughput, called multi-user diversity gain, that depends on the number of simultaneously connected users to the cell.

Chapter 04: Application and Results Analysis

This chapter presents the coverage prediction results obtained through the radio network planning tool for the area under study. The impact of massive MIMO technology is analyzed, for both single user and multi-user transmission, through coverage, quality and capacity predictions.

This main goal of this thesis is to study the impact of massive MIMO and beamforming. This study takes place in an urban and sub-urban environment, where the majority of these network improvement solutions will be implemented and the demand for more effective and advantageous data packet services increases each year.

In this way, the scenario where this study took place is the whole city of Oran, west of Algeria, of approximately 186.1 km^2. This scenario is mostly composed by a dense urban area, sub-urban, industrial and open spaces, followed by residential areas, few vegetation (despicable to path loss) and an open water area.

The analysis of every prediction will take into account the network coverage, capacity and quality, performed only for downlink. The predictions will be analyzed for single user MIMO and multi-user MIMO, depending on the different objectives proposed for evaluation. Both wireless technologies are targeted for improving the channel capacity, given that the SU-MIMO uses more than one transmission antenna to send different data streams (or layers) to the same user, whereas in MU-MIMO the layers are transmitted to different users.

Firstly, a comparison of every active antenna is made, to evaluate which active antenna can offer the best performance, also in **single user mode**.

Secondly, a comparison of every active antenna is made, however, with an increasing of the number of users in the cell, that is to say in **multi-user mode**.

Although the propagation model is empirical, it is important to mention that the algorithm used in this coverage predictions is deterministic, in other words, given a certain input, it will always produce the same output. Unless these input parameters are edited, the results are always the same, regardless of the number of simulations.

4.1 Comparison of AAS performance in SU-MIMO

In SU-MIMO (also called spatial multiplexing), the information is transmitted simultaneously over more than one data stream (or layer) using the same frequency/time resources to a single user. The three active antennas, AAS16, AAS32 and AAS64, are evaluated in order to understand which AAS is more advantageous in terms of network coverage, quality and capacity. When setting the prediction for a single user, it is possible to assess the performance of the massive MIMO antennas, since all the resources are allocated to a unique user. The most remarkable difference, that is known in advance, is the diversity in transmission of the AAS (16, 32 and 64 Tx antenna ports).

4.1.1 Network Coverage

The network coverage predictions predict the effective signal levels of different types of 5G NR in the area of study. The prediction is made by assessment of the reference signal SS-RSRP level. The graph in the figure 4.11 represents a Cumulative Distribution Function (CDF), where the resulting values are combined and shown along a curve. The figure represents the SS-RSRP cumulative area of the three AAS under study, succeeded by the mean SS-RSRP-DL value for each AAS given on table 4.4.

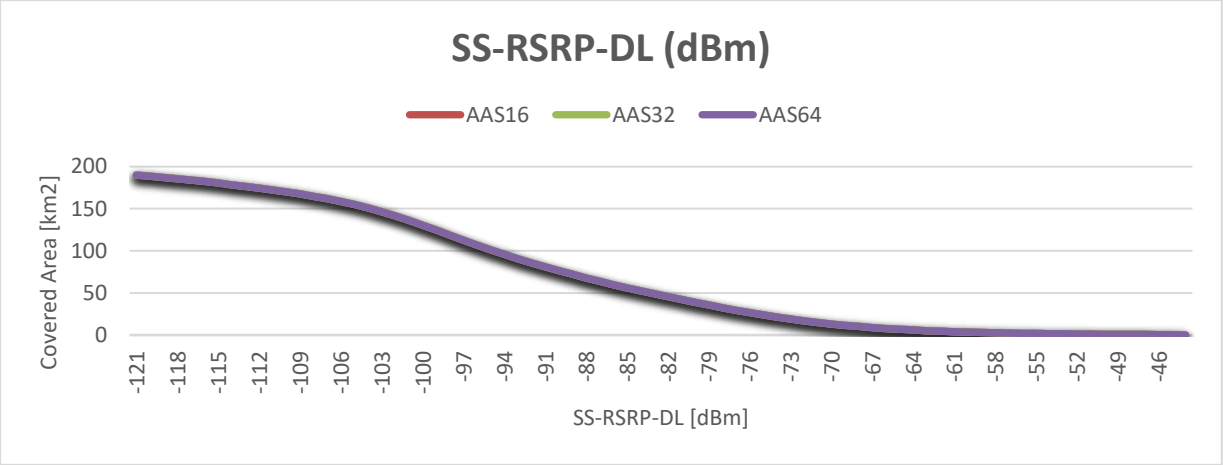


Figure 4.1: SS-RSRP-DL CDF by covered area.

	AAS16	AAS32	AAS64
Mean Value [dBm]	-91.46	-91.46	-91.46

Table 4.1: SS-RSRP-DL mean value per AAS coverage prediction.

Despite the difference in the number of TX/RX for each AAS, coverage is the same. The numbers of antenna ports in this study are equal to the number of antenna elements (refer to table 3.6) so no change will be seen in coverage due to no changes in antennas gain. **In real live network** conditions, some antenna elements can be combined in groups feeding a single port, so, the more antenna elements (radiating elements) in a specific port, the better the coverage due to the increased gain of the antenna.

4.1.2 Network Quality

Given that many sites were deployed without real traffic figures, the interference between cells based on coverage prediction and overlapping between covered areas is taken into account. The network quality coverage prediction is therefore determined by the PDSCH levels, which include also channel power allocation and the noise figure.

The PDSCH CINR coverage prediction is illustrated in figure 4.12 from the histogram generated. In the horizontal axis is represented the PDSCH CINR values in dB, and the covered area by each value in the vertical axis, in km^2.

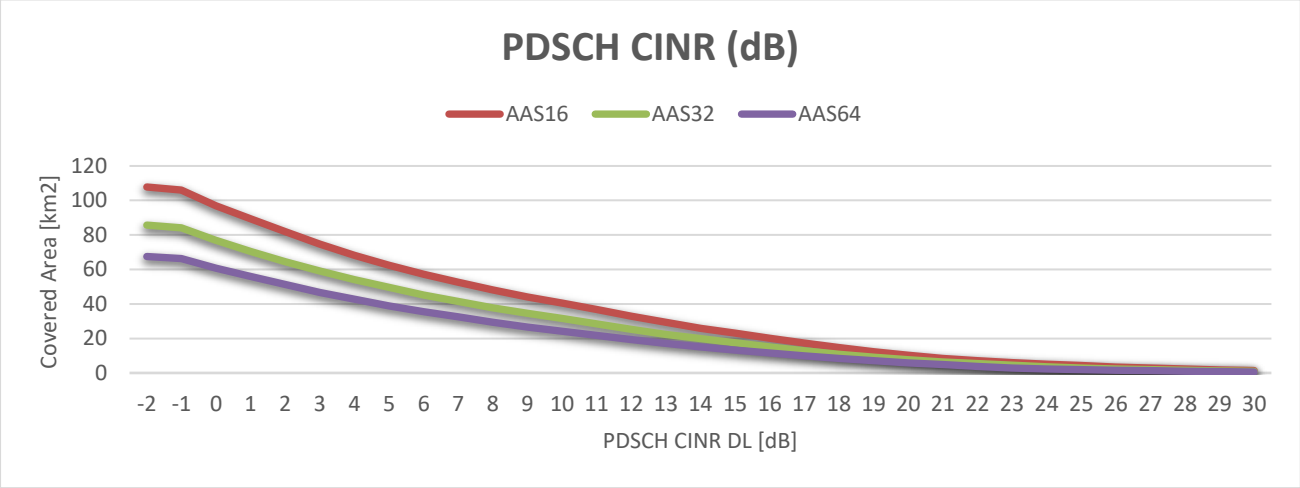


Figure 4.2: Frequency polygon of the PDSCH CINR level by covered area.

	AAS16	AAS32	AAS64
Mean Value [dB]	7.92	7.75	7.48

Table 4.2: Numerical results of the PDSCH CINR coverage prediction.

The results are expected as there are more antennas elements in AAS64 compared to ASS32 and to AAS16 as well, also we supposed that the number of power amplifiers is the same as the antennas elements, so the intercell interference will increase with MIMO TX/RX elements increase causing a CINR degradation as given on the table above. **In real live network**, if the user only has 4 RX (UE with MIMO support), the number of streams of the MIMO system is limited by the number of transmitting or receiving antennas, whichever is lower. Therefore, only 4 data streams will be received, so the results are in reality expected to be the same for every AAS in presence of real user traffic data.

4.1.3 Network Capacity

The CINR and bearer calculations for each pixel is the base of the channel throughput calculation. The bearer determination by CINR level provides which bearer efficiency is then multiplied by the total of symbols (i.e.; resource elements) in the DL radio frames.

The chart in figure 4.14 is a frequency polygon that represents the DL throughput values, represented on the horizontal axis, in Mbps, and the covered area on the vertical axis, in km2. The figure is succeeded by the table 4.6 with the numerical results of the DL throughput coverage prediction.

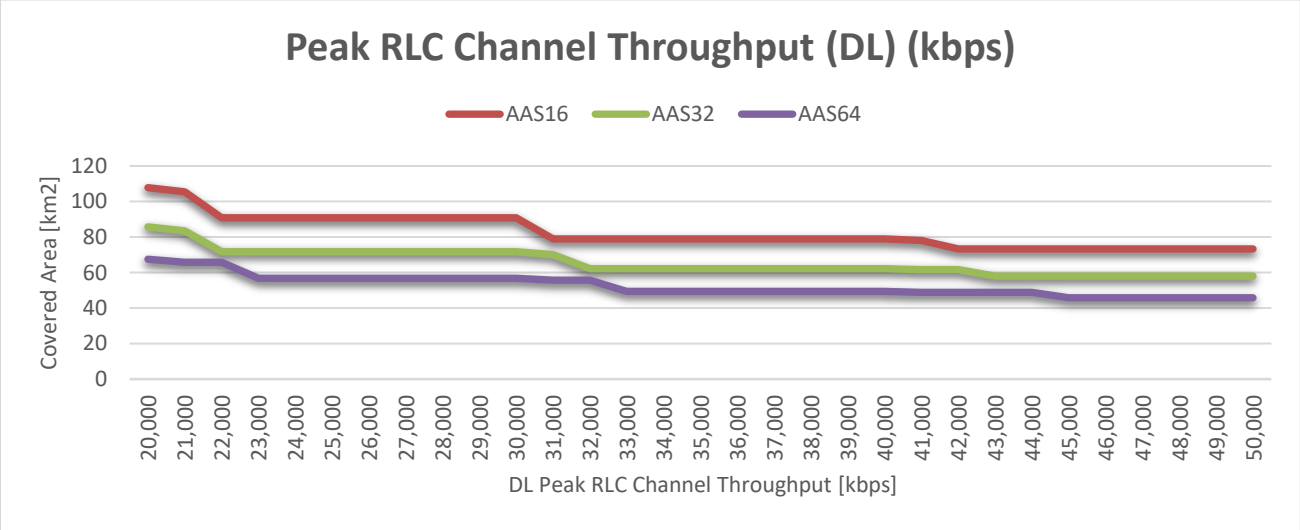


Figure 4.3: Frequency polygon of the cell capacity by covered area.

	AAS16	AAS32	AAS64
Mean Value [Mbps]	91.58	89.78	87.22

Table 4.3: Numerical results of the DL throughput coverage prediction.

Results expected in correlation to the CINR output as explained in the previous section, actually due to the selection of few sites covering a large area with less cells overlapping led to a such result (decreasing DL throughput with an increase of antennas elements). **In real live network** a single UE, using the same time/frequency resources has 16Tx in AAS16, 32Tx in AAS32 and 64Tx in AAS64. The utilization of larger number of antennas for signal transmission toward only one UE enables high degree of energy concentration in space as narrower beam is possible to be created. However, the receiver (UE) only has 4Rx antennas (UE with MIMO support). The use of spatial multiplexing with M transmission and N reception antenna ports can increase theoretically the throughput by M or N times, whichever is smaller. Simply put, the UE only has

4 reception antenna ports, which means no capacity gain and improvement will be achieved regardless of the high number of transmission antennas, because only 4 data streams will be received. This justifies the similar results obtained by every AAS, although the throughput performance of the AAS32 is slightly better, with higher mean value, and especially for throughputs above 550 Mbps, due to the also better CINR levels achieved previously. In this SU-MIMO case, the user throughput is equal to the cell throughput for the reason that all the resources are allocated towards one user.

4.2 Comparison of AAS performance in MU-MIMO

In MU-MIMO, data streams are distributed across multiple users on the same time/frequency resources, thus increasing the system capacity. It is highly supported by beamforming, in a way that the spatial focusing of beams in users spatially distributed maximizes the gain towards that UEs. It is only needed one receiving antenna port at the user equipment, unlike SU-MIMO.

In this study, 10 users were co-scheduled. Since the diversity support mode was set for MU-MIMO, the time/frequency resources will be multiplexed to the users by the scheduler in proportional fair mode, i.e., allocation of the same number of resources to all the users with a maximum throughput demand. The objective is to assess the impact of the diversity in the transmission antennas of AAS in MU-MIMO. All the AAS follow the same cell configurations previously mentioned in previous sections 3.3 and 3.5.

4.2.1 Network Coverage

The network coverage prediction is evaluated by the reference signal SS-RSRP. The figure 4.15 represents a graph of the SS-RSRP values in dBm, ranging from -121 dBm to more or equal than -43 dBm, over the covered area, in km^2. In other hand, there is a table providing the numerical results of the reference signal coverage prediction.

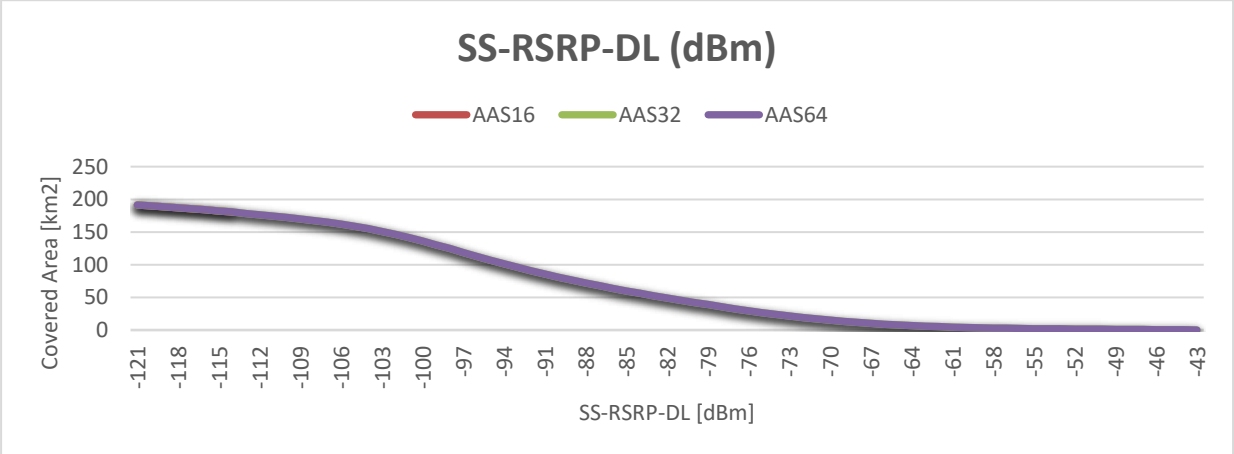


Figure 4.4: SS-RSRP CDF by covered area.

	AAS16	AAS32	AAS64
Mean Value [dBm]	-91.46	-91.46	-91.46

Table 4.4: Numerical results of the SS-RSRP coverage prediction.

It is observed the same SS-RSRP values as the previous study, in section 4.2.1. Although the number of Tx stands different for every AAS, the coverage is primarily influenced by the number of antenna elements and consequently by the antenna gain. These characteristics have remained the same, so it is natural to acquire the same output. The number of users does not influence the coverage, since the reference signal is calculated in every pixel, independently if the pixel represents one user or multiple users.

4.2.2 Network Quality

The network quality coverage prediction is assessed by the intercell interference based on the overlap between cells and the probability of collision between these cells. Figure 4.16 presents a CDF, where the horizontal axis represent the PDSCH CINR values, in dB, and the vertical axis represent the cumulative area in km^2, followed by the statistical results of the coverage prediction, exposed in table 4.8.

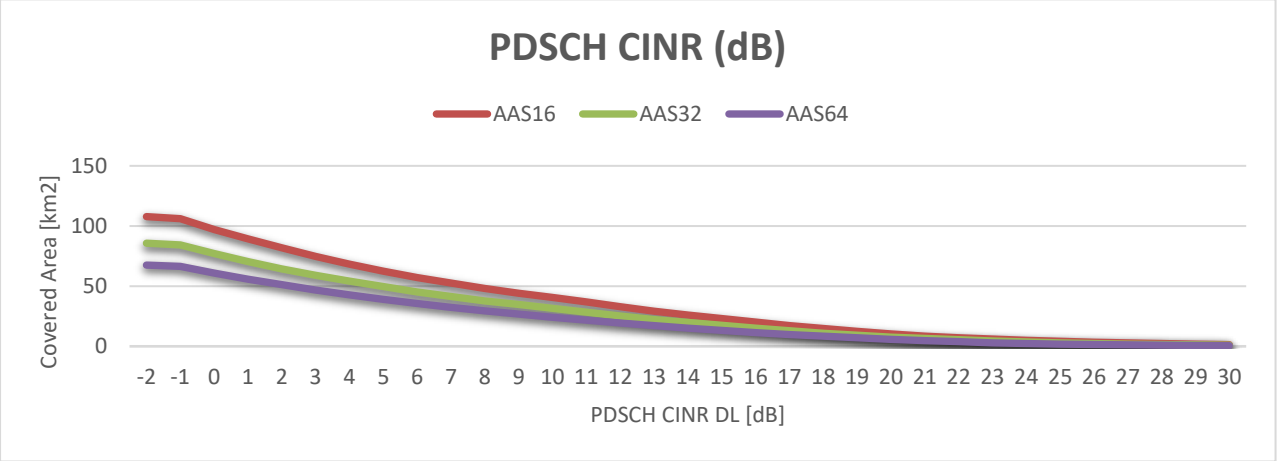


Figure 4.5: PDSCH CINR CDF by covered area.

	AAS16	AAS32	AAS64
Mean Value [dB]	8.63	8.44	8.31

Table 4.5: Numerical results of the PDSCH CINR coverage prediction.

The various data streams that each AAS can provide, can be used to serve different users simultaneously over the same time slot and frequency band. By accessing the channel state information, it is possible to encode the signals constructively by manipulating amplitudes and

phases in the desired directions. This way it is possible to mitigate interference between the users connected in the cell, increasing the CINR (compared to SU-MIMO). Since in this type of predictions there is no spatial distribution between the co-scheduled users, the radio planning tool applies a capacity gain in MU-MIMO configurations. Also, as explained on section 4.1.2 same behavior is observed regarding intercell interferences.

4.2.3 Network Capacity

The table below represents the mean DL throughputs for the different AAS, with the DL throughput values represented, it is clear that the AAS64 has higher cell capacity, the AAS64 achieved a throughput better than AAS16 and AAS32. It is clear that a capacity and multi-user gain was applied in every AAS by *Atoll*. These gains vary according to the number of users connected to the cell, the Tx/Rx pair set and the almost 30 radio bearers that can be selected, thereby the gains aren't constant.

	AAS16	AAS32	AAS64
Mean Value [MBps]	68.13	69.34	72.25

Table 4.6: Numerical results of the DL throughput coverage prediction.

In reality, independently of the gains applied by the network planning tool, it is expected that the increase in the number of transceivers results into an increase in cell capacity, due to the increase of independent data streams that are able to serve a greater number of users simultaneously, in the same bandwidth, thereby, increasing the spectral efficiency (bits/s/Hz). This fact is confirmed in the present study.

The per-user throughput in downlink could be calculated as a matter of curiosity, by dividing the downlink cell capacity by the number of DL users connected to cell, but, since the number of users connected is constant for every antenna prediction, dividing the cell capacity by 10 users would still show that the AAS64 could allocate more resources resulting in higher throughputs per user, highlighting the AAS64 the antenna with higher spectral efficiency and cell capacity.

General Conclusion

As given on the introduction, the main goal of this thesis was to study the impact of advanced antenna systems (massive MIMO and beamforming) in 5G-NR networks using *Atoll* through two analysis plans.

The First analysis, is a comparison of the MIMO performance between the three AAS under study (AAS16, AAS32 and AAS64), in terms of network coverage, quality and capacity, in single user mode. First, the network coverage is assessed, with similar results. Despite the difference in the number of Tx, the coverage is mostly influenced by the number of antenna elements (which is the same) and the antenna gain (which is the same). The network quality is then assessed, it is expected to achieve the same results, since the number of streams of the MIMO system is limited by the number of transmitting or receiving antennas, whichever is lower, so is limited by the 1 Rx of the UE, regardless of the number of Tx. Despite that, the results diverge due to the large area under evaluation and the number of sites studied, for future assessment and for stable results the chosen number of sites (cells) should be enough to made an continuous coverage layer with the best overlapping in order to get very accurate results.

Characterized by a link capacity, between the transmitter and the UE, which is as great as the number of parallel data streams transmitted. In a business view, and taking into account that the price of an active antenna increases with the complexity and number of transceivers, it is possible to obtain similar results through antennas that cost less, as is the case with AAS16.

The Second evaluation, present in the second section, switches its focus to MU-MIMO, also by comparing the performance between the three active antennas with respect to the network coverage, quality and capacity. Unlike SU-MIMO, MU-MIMO is characterized in terms of a capacity region, that is, the set of rates attainable for all UEs at the same time. 10 users per cell were co-scheduled, where the time/frequency resource were multiplexed to the different users.

The network coverage remained the same since it is chiefly influenced by the number of antenna elements and consequently by the antenna gain. The number of users does not influence the SS-RSRP levels since the signal is calculated for every pixel, regardless of how many users the pixel represent. In network quality, results were in correlation with the ones found in SU-MIMO, the intercell interferences were the main issue of degraded CINR which can be avoided in the future by increasing the number of sites (cells) and getting a continuous coverage layer with good overlapping. Regarding the network capacity, the AAS64 achieved the best cell downlink throughput, better than AAS16 and AAS32. It is expected that the increase in the number of transmission antenna ports, theoretically, lead to an increase of cell capacity and

spectral efficiency, due to the increase of independent data streams that are able to serve a greater number of users simultaneously. This fact is confirmed and shows to be the key to unlocking higher spectral efficiencies.

For future work, it is very important to get the maximum data regarding sites locations, number of cells, equipment used in the field including Tx/Rx units with their technical specifications and details, also the full data about antennas to be used with complete RF parameters to be set on site, cell and UE levels in order to be updated on the planning tool to get the maximum accurate results possible, at the end the field results will reflect how much the simulation was similar to real live network case.

Another interesting experiment would be the introduction of more than one cell, with high-frequency bands (mmWave), that is very promising and plays a crucial role in 5G. The comparison with other propagation models, preferably deterministic, could help to validate the empirical model present in this thesis.

References

[1] GSMA, “The State of Mobile Internet Connectivity,” 2019, last accessed June 2020. [Online]. Available: https://www.gsma.com/mobilefordevelopment/resources/References/the-state-of-mobile-internet-connectivity-report-2019/
[2] Nokia Bell Labs, “Who will satisfy the desire to consume?” last accessed June 2020. [Online]. Available: http://www.iot.gen.tr/wp-content/uploads/2017/03/160531-Nokia Bell Labs Mobility Traffic Report.pdf
[3] A. Osseiran, J. Monserrat, P. Marsch, O. Queseth, H. Tullberg, M. Fallgren, K. Kusume, A. Ha˜glund,
H. Droste, I. Leonardo Da Silva, P. Rost, M. Boldi, J. Sachs, P. Popovski, D. Gozalvez-Serrano, P. Fertl, Z. Li, F. Sanchez Moya, G. Fodor, and J. Lianghai, 5G Mobile and Wireless Communications Technology, 06 2016.
[4] A.-E. M. Taha, N. A. Ali, and H. S. Hassanein, LTE, LTE-advanced and WiMAX: Towards IMT-advanced Networks. John Wiley & Sons, 2011.
[5] A. Zaidi, F. Athley, J. Medbo, U. Gustavsson, G. Durisi, and X. Chen, 5G Physical Layer: Principles,
Models and Technology Components, 1st ed. Orlando, FL, USA: Academic Press, Inc., 2018.
[6] Ericsson, “5G Radio Access,” June 2014, last accessed June 2020. [Online]. Available: https://www.ericsson.com/49ec9f/assets/local/reports-papers/ericsson-technology-review/docs/2014/er-5g-radio-access.pdf
[7] IMT, “Framework and overall objectives of the future development of IMT for 2020 and beyond,” International Mobile Telecommunications (IMT), Technical Specification (TS), September 2015, last accessed June 2020. [Online]. Available: https://www.itu.int/dms pubrec/itu-r/rec/m/R-REC-M.2083-0-201509-I!!PDF-E.pdf
[8] Huawei Technologies Co. Ltd., “Huawei 5G Wireless Network Planning Solution White Paper,” 2018, last accessed June 2020. [Online]. Available: https://www-file.huawei.com/-/media/corporate/pdf/white%20paper/2018/5g wireless network planning solution en v2.pdf?la=en
[9] Ericsson, “Ericsson Mobility Report,” June 2019, last accessed June 2020. [Online]. Available: https://www.ericsson.com/49d1d9/assets/local/mobility-report/documents/2019/ericsson-mobility-report-june-2019.pdf
[10] A. Fragoso, “Impact of Massive MIMO Antennas on High Capacity 5G-NR Networks,” Master’s thesis, Instituto Superior Tecnico, 2019.
[11] S. Ahmadi, 5G NR: Architecture, Technology, Implementation, and Operation of 3GPP New Radio Standards. Elsevier Science, 2019.
[12] C. P. Shelton, “Coding for error detection and correction,” last accessed June 2020. [Online]. Available: https://users.ece.cmu.edu/∼koopman/des s99/coding/
[13] Y. Yuan and X. Wang, “5G New Radio: Physical Layer Overview,” ZTE Communications, vol. 1, 2017.
[14] Y. Cai, Z. Qin, F. Cui, G. Y. Li, and J. A. McCann, “Modulation and Multiple Access for 5G Networks,” 2017.
[15] A. A. Zaidi, R. Baldemair, H. Tullberg, H. Bjorkegren, L. Sundstrom, J. Medbo, C. Kilinc, and I. DaSilva, “Waveform and numerology to support 5g services and requirements,” IEEE Communications

Magazine, vol. 54, no. 11, pp. 90–98, November 2016.
[16] Claire Masterson, “Massive mimo and beamforming: The signal processing behind the 5g buzzwords,” Analog Dialogue, Tech. Rep., last accessed June 2020. [Online]. Available: https://www.analog.com/media/en/analog-dialogue/volume-51/number-3/articles/massive-mimo-and-beamforming-the-signal-processing-behind-the-5g-buzzwords.pdf
[17] J. Martins, “Impact of MIMO and Carrier Aggregation in LTE-Advanced,” Master’s thesis, Instituto Superior Tecnico, 2013.
[18] E. Dahlman, S. Parkvall, and J. Skold, 5G NR: The next generation wireless access technology. Academic Press, 2018.
[19] 3GPP, “Technical Specification Group Services and System Aspects; System Architecture for the 5G System,” 3rd Generation Partnership Project (3GPP), Technical Specification (TS) 23.501, 12 2018, version 15.4.0. [Online]. Available: https://www.3gpp.org/ftp/Specs/archive/23 series/23.501/
[20] Gabriel Brown, “Service-based architecture for 5g core networks,” Huawei, Tech. Rep., last accessed June 2020. [Online]. Available: https://img.lightreading.com/downloads/Service-Based-Architecture-for-5G-Core-Networks.pdf
[21] H. Holma, A. Toskala, and T. Nakamura, 5G Technology: 3GPP New Radio. Wiley, 2020.
[22] ONF, “Software-Defined Networking: The New Norm for Networks,” Open Networking Foundation, Tech. Rep., April 2012, last accessed June 2020. [Online]. Available: https://www.opennetworking.org/images/stories/downloads/sdn-resources/white-papers/wp-sdn-newnorm.pdf
[23] P. Gaj, M. Sawicki, G. Suchacka, and A. Kwiecien´, Computer Networks: 25th International Conference, CN 2018, Gliwice, Poland, June 19-22, 2018, Proceedings, ser. Communications in Computer and Information Science. Springer International Publishing, 2018.
[27] GSMA, “5G Implementation Guide,” July 2019, last accessed June 2020. [Online]. Available: https://www.gsma.com/futurenetworks/wp-content/uploads/2019/03/5G-Implementation-Guideline-v2.0-July-2019.pdf
[24] Wireless World Research Forum, “End to End Network Slicing,” Tech. Rep., 2017, last accessed June 2020. [Online]. Available: https://www.wwrf.ch/files/content%20wwrf/publications/outlook/Outlook21.pdf
[25] Tony Saboorian, “Network Slicing and 3GPP Service and Systems Aspects (SA) Standard,” last accessed April 2020. [Online]. Available: https://sdn.ieee.org/newsletter/december-2017/network-slicing-and-3gpp-service-and-systems-aspects-sa-standard
[26] 3GPP, “Study on new radio access technology: Radio access architecture and interfaces,” 3rd Generation Partnership Project (3GPP), Technical Specification (TS) 38.801, 3 2017, version 14.0.0. [Online]. Available: https://www.3gpp.org/ftp/Specs/archive/38 series/38.801/
[28] Harrison J Son, last accessed April 2020. [Online]. Available: https://www.netmanias.com/en/post/oneshot/14488/5g/5g-nsa-option-3a-3x-generic-operation
[29] Dave Morley, “Real-World Performance of 5G,” 2019, last accessed June 2020. [Online]. Available: https://www.nctatechnicalpapers.com/Paper/2019/2019-real-world-performance-of-5g/
[30] T. Curry and R. Abbas, “5G Coverage, Prediction, and Trial Measurements,” March 2020.
[31] J. H. Bae, A. Abotabl, H.-P. Lin, K.-B. Song, and J. Lee, “An overview of channel coding for 5G NR cellular communications,” APSIPA Transactions on Signal and Information Processing, vol.8,p. e17, 2019.
[32] Huawei Technologies Co. Ltd., “5G Spectrum - Public Policy Position.” [Online]. Avail-

able: https://www-file.huawei.com/-/media/CORPORATE/PDF/public-policy/public policy position 5g spectrum.pdf
[33] N. Chilamkurti, S. Zeadally, and H. Chaouchi, Next-Generation Wireless Technologies: 4G and Beyond, ser. Computer Communications and Networks. Springer London.
[34] 3GPP, "Physical channels and modulation," 3rd Generation Partnership Project (3GPP), Technical Specification (TS) 38.211, 6 2019, version 15.6.0. [Online]. Available: https://www.3gpp.org/ftp/Specs/archive/38 series/38.211/
[35] M. Sriharsha, S. Dama, and K. Kuchi, "A complete cell search and synchronization in LTE," Eurasip Journal on Wireless Communications and Networking, vol. 2017, 12 2017.
[36] B. Bertenyi, S. Nagata, H. Kooropaty, X. Zhou, W. Chen, Y. Kim, X. Dai, and X. Xu, "5G NR radiointerface," Journal of ICT Standardization, vol. 6, no. 1, pp. 31–58, 2018.
[37] Keysight, last accessed April 2020. [Online]. Available: https: //ujg433eawlo3i4uqknhm8e1b-wpengine.netdna-ssl.com/wp-content/uploads/2018/09/Keysight3.png
[38] D. Pinchera, M. D. Migliore, F. Schettino, and G. Panariello, "Antenna Arrays for Line-of-Sight Massive MIMO: Half Wavelength is not Enough," arXiv e-prints, p. arXiv:1705.06804, May 2017.
[39] GSMA, "5G Spectrum - Public Policy Position," March 2020, last accessed June 2020. [Online]. Available: https://www.gsma.com/spectrum/wp-content/uploads/2020/03/5G-Spectrum-Positions.pdf
[40] A. A. Zaidi, R. Baldemair, V. Moles-Cases, N. He, K. Werner, and A. Cedergren, "Ofdm numerology design for 5g new radio to support iot, embb, and mbsfn," IEEE Communications Standards Magazine, vol. 2, no. 2, pp. 78–83, June 2018.
[41] R. Rios, "5G Network Planning and Optimization using Atoll," Master's thesis, Escola Te`cnica d'Enginyeria de Telecomunicacio´ de Barcelona, 2019.
[42] 5G Americas, "Advanced antenna systems for 5G networks," Tech. Rep., 2019, last accessed June 2020. [Online]. Available: https://www.5gamericas.org/wp-content/uploads/2019/ 08/5G-Americas Advanced-Antenna-Systems-for-5G-White-Paper.pdf
[43] D. Anzaldo, "LTE-Advanced Release-12 shapes new eNodeB transmitter Architecture: Part 1, Technology Evolution." [Online]. Available: https://www.maximintegrated.com/en/design/ technical-documents/app-notes/6/6062.html
[44] L. Liu, R. Chen, S. Geirhofer, K. Sayana, Z. Shi, and Y. Zhou, "Downlink MIMO in LTE-advanced:
SU-MIMO vs. MU-MIMO," IEEE Communications Magazine, vol. 50, no. 2, pp. 140–147, February 2012.
[45] Ericsson, "Advanced antenna systems for 5G networks," Tech. Rep., 2019, last accessed June 2020. [Online]. Available: https://www.ericsson.com/4a8a87/assets/local/reports-papers/ white-papers/10201407 wp advanced antenna system nov18 181115.pdf
[46] Keith Benson, "Phased Array Beamforming ICs Simplify Antenna Design," 2019, last accessed June 2020. [Online]. Available: https://www.analog.com/media/en/analog-dialogue/volume-53/ number-1/phased-array-beamforming-ics-simplify-antenna-design.pdf
[47] I. Ahmed, H. Khammari, A. Shahid, A. Musa, K. S. Kim, E. De Poorter, and I. Moerman, "A survey on hybrid beamforming techniques in 5g: Architecture and system model perspectives," IEEE Communications Surveys Tutorials, vol. 20, no. 4, pp. 3060–3097, 2018.
[48] H. Halbauer, S. Saur, J. Koppenborg, and C. Hoek, "3D beamforming: Performance improvement for cellular networks," Bell Labs Technical Journal, vol. 18, no. 2, pp. 37–56, 2013.
[49] C. Shepard, H. Yu, N. Anand, E. Li, T. Marzetta, R. Yang, and L. Zhong, "Argos: practical many antenna base stations," August 2012.

[50] M. D. Pappa, C. Ramesh, and M. N. Kumar, “Performance comparison of massive MIMO and conventional MIMO using channel parameters,” 2017 International Conference on Wireless Communications, Signal Processing and Networking (WiSPNET), pp. 1808–1812, 2017.
[51] Y. Wu, J. W. M. Bergmans, and S. Attallah, “Effects of Antenna Correlation and Mutual Coupling on the Carrier Frequency Offset Estimation in MIMO Systems,” in 2010 6th International Conference on Wireless Communications Networking and Mobile Computing (WiCOM), 2010, pp. 1–4.
[52] N. H. M. Adnan, I. M. Rafiqul, and A. H. M. Z. Alam, “Effects of inter element spacing on large antenna array characteristics,” in 2017 IEEE 4th International Conference on Smart Instrumentation,
Measurement and Application (ICSIMA), 2017, pp. 1–5.
[53] P. Delos, “Physical Size Allocations for RF Electronics in Digital Beamforming
Phased Arrays,” Analog Devices, Inc., Tech. Rep., 2018, last accessed June 2020.
[Online]. Available: https://www.analog.com/media/en/technical-documentation/tech-articles/A38400-Physical-Size-Allocations-for-RF-Electronics-in-Digital-Beamforming-Phased-Arrays.pdf
[54] J. M. Vella and S. Zammit, “Performance improvement of long distance MIMO links using cross polarized antennas,” in Melecon 2010 - 2010 15th IEEE Mediterranean Electrotechnical Conference, 2010, pp. 1287–1292.
[55] J.-K. Hong, “Performance Analysis of Dual-Polarized Massive MIMO System with Human-Care IoT
Devices for Cellular Networks,” J. Sensors, vol. 2018, pp. 3 604 520:1–3 604 520:8, 2018.
[56] C.-X. Wang, S. Wu, L. Bai, X. You, J. Wang, and I. Chih-Lin, “Recent advances and future challenges for massive MIMO channel measurements and models,” Science China Information Sciences, vol. 59, no. 2, pp. 1–16, 2016.
[57] J. Flordelis, F. Rusek, F. Tufvesson, E. G. Larsson, and O. Edfors, “Massive MIMO Performance-TDD Versus FDD: What Do Measurements Say?” IEEE Transactions on Wireless Communications, vol. 17, no. 4, pp. 2247–2261, April 2018.
[58] J. Medbo, P. Kyosti, K. Kusume, L. Raschkowski, K. Haneda, T. Jamsa, V. Nurmela, A. Roivainen,
and J. Meinila, “Radio propagation modeling for 5G mobile and wireless communications,” IEEE Communications Magazine, vol. 54, no. 6, pp. 144–151, June 2016.
[59] A. Iodice, D. Riccio, and G. Ruello, “The role of propagation software tools for planning 5G wireless networks,” 5Gitaly, 2019.
[60] G. Gougeon, Y. Corre, and M. Z. Aslam, “Ray-based Deterministic Channel Modelling for sub-THz Band,” in 2019 IEEE 30th International Symposium on Personal, Indoor and Mobile Radio Communications (PIMRC Workshops), Sep. 2019, pp. 1–6.
[61] C. Wang, J. Bian, J. Sun, W. Zhang, and M. Zhang, “A Survey of 5G Channel Measurements and Models,” IEEE Communications Surveys Tutorials, vol. 20, no. 4, pp. 3142–3168, 2018.
[62] L. M. Correia, “Mobile Communication Systems - Course Notes,” IST, 2014.
[63] Visicom, last accessed April 2020. [Online]. Available: https://visicom.ua/products/data for wireless planning?lang=en
[64] Forsk, “Atoll Wireless Network Engineering Software, v3.4,” 2019, last accessed June 2020.
[Online]. Available: https://www.forsk.com/sites/default/files/atoll 3 4 light.pdf